Heat transfer analysis of MHD viscous fluid in a ciliated tube with entropy generation

Name: Salman Akhtar
Reg. # 00000203349

A dissertation submitted in partial fulfillment of the requirements for the degree of
Master of Philosophy in
Mathematics

Supervised by: Dr. Noreen Sher Akbar
Department of Mathematics
School of Natural Sciences (SNS)
National University of Sciences and Technology (NUST),
Islamabad, Pakistan

2019

FORM TH-4

National University of Sciences & Technology

MS THESIS WORK

We hereby recommend that the dissertation prepared under our supervision by: Salman Akhtar, Regn No. 00000203349 Titled: **Heat transfer analysis of MHD viscous fluid in a ciliated tube with entropy Generation** accepted in partial fulfillment of the requirements for the award of MS degree.

Examination Committee Members

1. Name: DR. MUHAMMAD ASIF FAROOQ Signature: MAsif

2. Name: DR. SYED TAYYAB HUSSAIN SHAH Signature: Tayyab Hussain 30/5/19

External Examiner: DR. RAHMAT ELLAHI Signature:

Supervisor's Name DR. NOREEN SHER AKBAR Signature:

Head of Department

30/5/2019
Date

COUNTERSINGED

Date: 30/05/19

Dean/Principal

THESIS ACCEPTANCE CERTIFICATE

Certified that final copy of MS thesis written by **Mr. Salman Akhtar** (Registration No. **00000203349**), of **School of Natural Sciences** has been vetted by undersigned, found complete in all respects as per NUST statutes/regulations, is free of plagiarism, errors, and mistakes and is accepted as partial fulfillment for award of MS/M.Phil degree. It is further certified that necessary amendments as pointed out by GEC members and external examiner of the scholar have also been incorporated in the said thesis.

Signature: ____________________

Name of Supervisor: Dr. Noreen Sher Akbar

Date: 30/05/19

Signature (HoD): ____________________

Date: 30/05/2019

Signature (Dean/Principal): ____________________

Date: 30/05/19

In the name of ALLAH, the Gracious, the Merciful

Dedicated to

My respected parents, my loving sisters and brothers

Acknowledgements

First of all, I would like to thank **Allah Almighty**, who has given me the ability, courage and His blessings to complete this thesis. He gave me strength and right path throughout my research work.

My special and sincere thanks to my supportive supervisor, **Dr. Noreen Sher Akbar** for providing me the most peaceful environment to work and guiding me throughout my research work. A special thanks to my guidance and evaluation committee members, **Dr. M. Asif Farooq** and **Dr. Syed Tayyab Hussain Shah**, for their valuable guidance, suggestions and encouragement. I am grateful especially to **School of Natural Sciences**, **NUST** for providing me all the facilities and a platform to work. I greatly acknowledge the facilities and technical support provided by other schools of NUST.

Salman Akhtar

Abstract

In fluid dynamics, the study of fluid's velocity, temperature, pressure, dynamic viscosity and momentum have significant importance. This work explains the systematic study of creeping flow, in a horizontal porous tube containing cilia, due to metachronal wave propagation. Since heat transfer study has huge importance in various biomedical and biological industry problems. This work also includes the mathematical study of transfer of heat and entropy generation analysis of MHD viscous fluid in a tube containing cilia. The metachronal wave propagation is main cause behind this creeping viscous flow. In both problems, a low Reynolds number is used as the inertial forces are weaker than viscous forces and also creeping flow limitations are fulfilled. For cilia movement, a very large wavelength of metachronal wave is taken into account. The heat transfer for the flow of MHD viscous fluid is examined by entropy generation. Numerical solutions are calculated by using mathematica. Exact mathematical solutions are produced for the governing equations and analyzed with the help of graphs. Streamlines are also plotted.

Contents

1 Introduction………………………………………………………………….. **1**

2 A Study on Creeping viscous flow through a ciliated porous tube

2.1 **Introduction**…………………………………………………………………. **5**

2.2 **Mathematical model**…………………………………………………. **6**

2.3 **Numerical results and discussion**……………………………….. **10**

3 Heat transfer analysis of MHD viscous fluid in a ciliated tube with entropy generation

3.1 **Introduction**………………………………………………………………….. **22**

3.2 **Mathematical formulation**………………………………………….. **23**

3.3 **Viscous dissipation and Entropy generation**………………….. **26**

3.4 **Exact solutions**….……………………………………………………… **27**

3.5 Results and discussion…………………………………………………. **28**

References………………………………………………………………….. **41**

Chapter 1

Introduction

The mechanism in which heat transmits from high temperature reservoir to low temperature reservoir is called heat transfer. It occurs, because of temperature discrimination between the system and its encircling, across the boundary of the system. It may occur inside the system because of temperature variation at various points within the system. The potential behind this heat flow is the difference in temperature. Biological propulsion has many applications in medicine, aerospace and it is attaining the attraction of many scientists because of its significant uses. Different mathematical researches have been conducted for many living things at various length scales and Reynolds number. Wu [1] has given the most radiant study of the subject. The area of his research includes flows for both microscopic organisms as well as huge marine mammals . Cilia[1] propulsion is of great importance at microscopic level. As explained by Wu [2], this field of biological hydrodynamic propulsion has been attracting the interest of many researchers for decades. In case of sperm flagella of few insects, the span of cilia ranges from a few microns to more than 2 mm. Cilia have been set up as beating with a whip-like irregular mechanism which contains both a prevailing as well as recovery stroke. Metachronal waves are generated because of collective beating of many cilia. When the metachronal wave and effective stroke both are parallel then it is termed as symplectic otherwise antiplectic. As illustrated by Feng and Cho [3], In many bio-inspired engineering systems and bio-mimetics, these characteristics have attracted attention of many scientists and researchers especially in nanomedicine and drug delivery. In general, atmost two long flagella are present in a cell whereas several cilia are present in ciliated cells. For example, only a single flagellum is present

[1] Cilia are hair-like structures that protrude from the surfaces of certain organisms and deform in a wavelike fashion to transport fluids.

in mammalian spermatozoa, two flagella in unicellular green alga Chlamydomonas and a few thousand cilia are present in unicellular protozoan Paramecium. There purpose is both nutrition and locomotion. The linear stokes equations, with no slip at the walls, are used to control the motion of cilia and flagella [4]. Sleigh [5] has described systematically the formation of cilia, facts by which motion of cilia is affected and the integrate beating of cilia. In male reproductive tract, the impact of cilia on flow rates is studied by Lardner and Shack [6]. Blake [7] developed a mathematical model that explains the microscopic structure for ciliated organisms. The fluid mechanism of cilia motion is theoretically studied by Wu [8]. For cilia movement, the oscillatory thin boundary layer theory is presented by Brennen [9]. Moreover, water movement by cilia is studied by Sleigh and Aiello [10]. The fluid flow, by cilia transport, with variable viscosity is investigated by Agarwal and Uddin [11]. For cilia movement, a spherical container approach is developed by Blake [12]. The flow of Newtonain fluids developed by mechanical cilia oscillations is studied by Miller [13]. For cilia-produced mucous flow, Barton and Raynor [14] developed a systematic approach. The impacts for the flow of viscoelastic fluid on cilia movement are studied by Smith et al [15]. A fluid-structure interaction view point for the hydrodynamics of cilia movement is studied by Dauptain et al [16]. Three dimensional computations for cilia movements are presented by Khaderi and Onck [17]. Khaderi et al [18] studied a flow in which forward and backward motion of artificial cilia is not same. For microfluidic propulsion, the study on magnetically-pushed artificial cilia is reported by Khaderi et al [19]. Recently, In biological porous media, the transport phenomena has attracted much attention. Human body organs like kidneys, tissues, lungs and our skin consist of permeable materials [20]. A medium having many tiny holes spread over the matter is called porous media [21]. Khaled and Vafai [22] have studied the convective flow models for porous media. Staffman [23] presented an example for flow having boundary conditions described for porous medium.

Peristalsis is a stimulating fluid flow problem in a media having pours. Peristalsis is a wavelike movement that is generated by regular contraction as well as relaxation of neighbouring locations. The flow developed because of peristaltic reflex in an isolated guinea pig ileum is studied by Jeffrey et al [24]. The peristaltic flow through an asymmetric porous media is explained by Elshehawey et al [25]. Recent study on peristaltic move of Newtonian as well as non-Newtonian fluids in magnetohydrodynamics is developed by Tripathi and Beg [26].

In a closed thermodynamic system, entropy occurs due to restlessness in a system . It is the measure of disorder of the system. Entropy of a system varies inversely with the temperature and directly with reversible variation in heat. The entropy generation analysis with transfer of heat is studied by Bejan [27]. Pakdemirli and Yilbas [28] discussed the entropy generation due to flow of a non-Newtonian fluid in a tube. In backward facing step flow, Nada [29] examined the entropy generation due to heat and fluid flow for various expansion ratios. In laminar flow through the hexagonal cross-sectional pipe having persistent temperature at walls, entropy generation has been studied by Oztop et al [30]. Relevant study on entropy is given in Ref. [31-41].

A precise analysis of mathematical research has revealed that the study of transfer of heat for magnetohydrodynamic viscous fluid in a ciliated tube with entropy generation is not studied mathematically. This research includes the study of heat transfer for MHD viscous fluid in a ciliated tube with entropy generation. Exact mathematical solutions are developed for the differential equation problem and are examined with the help of graphs.

Chapter 2

A Study on creeping viscous flow through a ciliated porous tube

2.1. Introduction:

This chapter includes the study of creeping[2] viscous flow, in a horizontal porous[3] tube containing cilia, due to metachronal wave propagation. A low Reynolds number is used as the inertial forces are weaker than viscous forces and also creeping flow limitations are fulfilled. For cilia movement, a very large wavelength of metachronal wave is taken into account. Mathematical solutions have been obtained for the governing equations. To estimate and elaborate numerical results, Mathematica software is used. The affect of Darcy number and slip parameter on velocity of fluid, trapping of bolus and pressure gradient are studied graphically. The trapping of bolus rises as the value of slip parameter increases. This work is useful for organic propulsion of scientific micro machines in drug transport.

2.2. Mathematical model

[2] Creeping flow is a flow in which inertial forces are weaker than viscous forces.

[3] A medium having tiny holes dispersed throughout the matter is called porous medium.

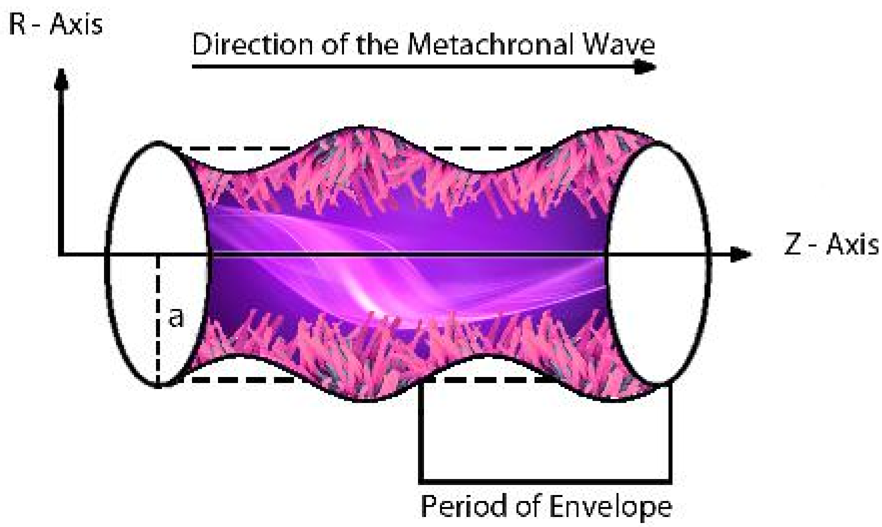

Figure 1 : Geometry of the problem [47]

Consider an incompressible[4] Newtonian fluid flow in a ciliated tube. The flow is produced because of integrate beating of cilia and there is hydrodynamic slip at walls. The internal side of the tube contains cilia and metachronal[5] waves are generated because of integrate functioning of cilia. Then pick out the cylindrical coordinate system $(\overline{R},\overline{Z})$, wherein the $\overline{Z}$ -axis is oriented alongside the significant line of pipe having $\overline{R}$ -axis perpendicular to it. Cilia show wave movement with pace, c, alongside the outer wall. The envelope of cilia pointers are described mathematically as [1,9]

$$\overline{R} = \overline{H} = \bar{f}(\overline{Z},\bar{t}) = a + a\varepsilon\cos\left(\frac{2\pi}{\lambda}(\overline{Z} - c\bar{t})\right),$$
$$\overline{Z} = \overline{g}(\overline{Z},\overline{Z}_0,\bar{t}) = a + a\varepsilon\alpha\sin\left(\frac{2\pi}{\lambda}(\overline{Z} - c\bar{t})\right), \quad (1)$$

[4] Incompressible flow is a flow in which fluid density is constant.

[5] Metachronal wave is developed because of sequential action of structures like cilia.

Here ε is cilia length parameter, a shows radius of tube, λ depicts wavelength, c represents velocity of the wave, α is eccentricity for elliptic movement and $\overline{Z}$ is the reference location of particle.

The velocities are given as

$$\overline{W} = \left(\frac{\partial \overline{Z}}{\partial \bar{t}}\right)_{\overline{Z}_0} = \frac{\partial \bar{g}}{\partial \bar{t}} + \frac{\partial \bar{g}}{\partial \overline{Z}}\frac{\partial \overline{Z}}{\partial \bar{t}} = \frac{\partial \bar{g}}{\partial \bar{t}} + \frac{\partial \bar{g}}{\partial \overline{Z}}\overline{W},$$
$$\overline{U} = \left(\frac{\partial \overline{R}}{\partial \bar{t}}\right)_{\overline{Z}_0} = \frac{\partial \bar{f}}{\partial \bar{t}} + \frac{\partial \bar{f}}{\partial \overline{Z}}\frac{\partial \overline{Z}}{\partial \bar{t}} = \frac{\partial \bar{f}}{\partial \bar{t}} + \frac{\partial \bar{f}}{\partial \overline{Z}}\overline{W}, \tag{2}$$

Using eq. (2) in eq. (1), we have

$$\overline{W} = \frac{-(2\pi/\lambda)[\varepsilon\alpha a c\cos(2\pi/\lambda)(\overline{Z}-c\bar{t})]}{[1-(2\pi/\lambda)\{\varepsilon\alpha a\cos(2\pi/\lambda)(\overline{Z}-c\bar{t})\}]},$$
$$\overline{U} = \frac{(2\pi/\lambda)[\varepsilon a c\sin(2\pi/\lambda)(\overline{Z}-c\bar{t})]}{[1-(2\pi/\lambda)\{\varepsilon\alpha a\cos(2\pi/\lambda)(\overline{Z}-c\bar{t})\}]}, \tag{3}$$

The flow is transient for fixed coordinates $(\overline{R},\overline{Z})$, but it is regular for moving frame $(\bar{r},\bar{z})$ whereas speed of flow is same for both frames. The equations for viscous flow in wave frame are

Continuity equation:

$$\frac{1}{\overline{R}}\frac{\partial(\overline{R}\,\overline{U})}{\partial \overline{R}} + \frac{\partial \overline{W}}{\partial \overline{Z}} = 0, \tag{4}$$

R-direction momentum equation:

$$\rho\left[\frac{\partial\overline{U}}{\partial\bar{t}}+\overline{U}\,\frac{\partial\overline{U}}{\partial\overline{R}}+\overline{W}\,\frac{\partial\overline{U}}{\partial\overline{Z}}\right]=-\frac{\partial\overline{P}}{\partial\overline{R}}+\mu\frac{\partial}{\partial\overline{R}}\left[2\frac{\partial\overline{U}}{\partial\overline{R}}\right]+\mu\frac{2}{\overline{R}}\left(\frac{\partial\overline{U}}{\partial\overline{R}}-\frac{\overline{U}}{\overline{R}}\right)+\mu\frac{\partial}{\partial\overline{Z}}\left[\frac{\partial\overline{U}}{\partial\overline{R}}+\frac{\partial\overline{W}}{\partial\overline{Z}}\right], \quad (5)$$

Z-direction momentum equation:

$$\rho\left[\frac{\partial\overline{W}}{\partial\bar{t}}+\overline{U}\,\frac{\partial\overline{W}}{\partial\overline{R}}+\overline{W}\,\frac{\partial\overline{W}}{\partial\overline{Z}}\right]=-\frac{\partial\overline{P}}{\partial\overline{Z}}+\mu\frac{\partial}{\partial\overline{Z}}\left[2\frac{\partial\overline{W}}{\partial\overline{Z}}\right]+\mu\frac{1}{\overline{R}}\frac{\partial}{\partial\overline{R}}\left[\overline{R}\left(\frac{\partial\overline{U}}{\partial\overline{Z}}+\frac{\partial\overline{W}}{\partial\overline{R}}\right)\right]-\frac{\mu}{\mathrm{K}}\overline{W}, \quad (6)$$

The shift between the fixed and moving frames:

$$\begin{gathered}\bar{r}=\overline{R},\quad \bar{z}=\overline{Z}-c\bar{t},\quad \bar{u}=\overline{U},\\ \overline{w}=\overline{W}-c,\quad \overline{p}(\bar{z},\bar{r})=\overline{P}(\overline{Z},\overline{R},\bar{t}),\end{gathered} \quad (7)$$

Now using these transformations in above equations, we obtain these equations:

$$\frac{1}{\bar{r}}\frac{\partial(\bar{r}\bar{u})}{\partial\bar{r}}+\frac{\partial\overline{w}}{\partial\bar{z}}=0, \quad (8)$$

$$\rho\left[\bar{u}\,\frac{\partial\bar{u}}{\partial\bar{r}}+\overline{w}\,\frac{\partial\bar{u}}{\partial\bar{z}}\right]=-\frac{\partial\overline{P}}{\partial\bar{r}}+\mu\frac{\partial}{\partial\bar{r}}\left[2\frac{\partial\bar{u}}{\partial\bar{r}}\right]+\mu\frac{2}{\bar{r}}\left(\frac{\partial\bar{u}}{\partial\bar{r}}-\frac{\bar{u}}{\bar{r}}\right)+\mu\frac{\partial}{\partial\bar{z}}\left[\frac{\partial\bar{u}}{\partial\bar{r}}+\frac{\partial\overline{w}}{\partial\bar{z}}\right], \quad (9)$$

$$\rho\left[\bar{u}\,\frac{\partial\overline{w}}{\partial\bar{r}}+\overline{w}\,\frac{\partial\overline{w}}{\partial\bar{z}}\right]=-\frac{\partial\overline{P}}{\partial\bar{z}}+\mu\frac{\partial}{\partial\bar{z}}\left[2\frac{\partial\overline{w}}{\partial\bar{z}}\right]+\mu\frac{1}{\bar{r}}\frac{\partial}{\partial\bar{r}}\left[\bar{r}\left(\frac{\partial\bar{u}}{\partial\bar{z}}+\frac{\partial\overline{w}}{\partial\bar{r}}\right)\right]-\frac{\mu}{\mathrm{K}}(\overline{w}+c), \quad (10)$$

Ellahi et al. [42], Sadaf and Nadeem [46] have described the relevant conditions on boundaries.

$$\frac{\partial \overline{w}}{\partial \overline{r}} = 0, \quad \text{at} \quad r = 0,$$
$$w = -1 - \frac{2\pi\varepsilon\alpha\beta\cos(2\pi z)}{1 - 2\pi\varepsilon\alpha\beta\cos(2\pi z)} - \frac{\mathrm{K}}{\alpha_1 *}\frac{\partial \overline{w}}{\partial \overline{r}}, \quad \text{at} \quad r = \overline{h}(z). \tag{11}$$

Where $2\pi\varepsilon\alpha\beta\cos(2\pi z)/[1 - 2\pi\varepsilon\alpha\beta\cos(2\pi z)]$ is the cilia factor.

The dimensionless variables are described as

$$r = \frac{\overline{r}}{a}, \quad z = \frac{\overline{z}}{\lambda}, \quad w = \frac{\overline{w}}{c}, \quad u = \frac{\lambda\overline{u}}{ac}, \quad p = \frac{a^2\overline{p}}{c\lambda\mu},$$
$$\beta = \frac{a}{\lambda}, \quad D_a = \frac{\mathrm{K}}{a^2}, \quad \alpha_1 = \frac{\alpha_1 *}{a}. \tag{12}$$

Now using the above variables in equations (9) and (10), also applying the estimation of large wavelength and small Reynolds number[6], the dimensionless equations are given as

$$\frac{\partial p}{\partial r} = 0, \tag{13}$$
$$\frac{\mathrm{dp}}{\mathrm{dz}} = \frac{1}{r}\frac{\partial}{\partial r}\left(r\frac{\partial w}{\partial r}\right) - \frac{1}{D_a}(w+1), \tag{14}$$

The dimensionless conditions on boundaries are described by

$$\frac{\partial w}{\partial r} = 0, \quad \text{at} \quad r = 0, \tag{14a}$$
$$w = -1 - \frac{2\pi\varepsilon\alpha\beta\cos(2\pi z)}{1 - 2\pi\varepsilon\alpha\beta\cos(2\pi z)} - \frac{\sqrt{D_a}}{\alpha_1}\frac{\partial w}{\partial r},$$
$$\text{at} \quad r = h(z) = 1 + \varepsilon\cos(2\pi z). \tag{14b}$$

[6] Reynolds number shows in case the flow is laminar or irregular. It is defined as the ratio of inertial forces to viscous forces.

Integrating equation (14) and applying relevant conditions on boundaries, the velocity profile is calculated as

$$w(r,z) = -1 - D_a \frac{dp}{dz} + \frac{\alpha_1[D_a(dp/dz) - 2\pi\varepsilon\alpha\beta\cos(2\pi z)/(1-2\pi\varepsilon\alpha\beta\cos(2\pi z))]I_0(r/\sqrt{D_a})}{I_1(h/\sqrt{D_a}) - I_0(h/\sqrt{D_a})}, \quad (15)$$

The flow rate (F) is

$$F = 2\pi\int_0^h rw\mathrm{d}r. \quad (16)$$

Solving equation (16), we have

$$\frac{dp}{dz} = \frac{\frac{I_1(h/\sqrt{D_a})\left((2\pi\varepsilon\alpha\beta\cos(2\pi z)-1)(F+\pi h^2) - 2\pi\alpha_1\sqrt{D_a}hn\right)}{2\pi\varepsilon\alpha\beta\cos(2\pi z)-1} - (F+\pi h^2)I_0(h/\sqrt{D_a})}{\pi D_a h\left(hI_0(h/\sqrt{D_a}) - (h-2\alpha_1\sqrt{D_a})I_1(h/\sqrt{D_a})\right)}, \quad (17)$$

Flow rates for both frames have been linked by:

$$Q = F + \frac{1}{2}\left(1+\frac{\varepsilon^2}{2}\right). \quad (18)$$

The rise in pressure (ΔP) is obtained as:

$$\Delta P = \int_0^1 \frac{dp}{dz}\mathrm{d}z. \quad (19)$$

2.3. Numerical results and discussion:

This segment describes the velocity field, pressure gradient, flow rate Q and streamlines for numerous physical parameters with the help of graphs.

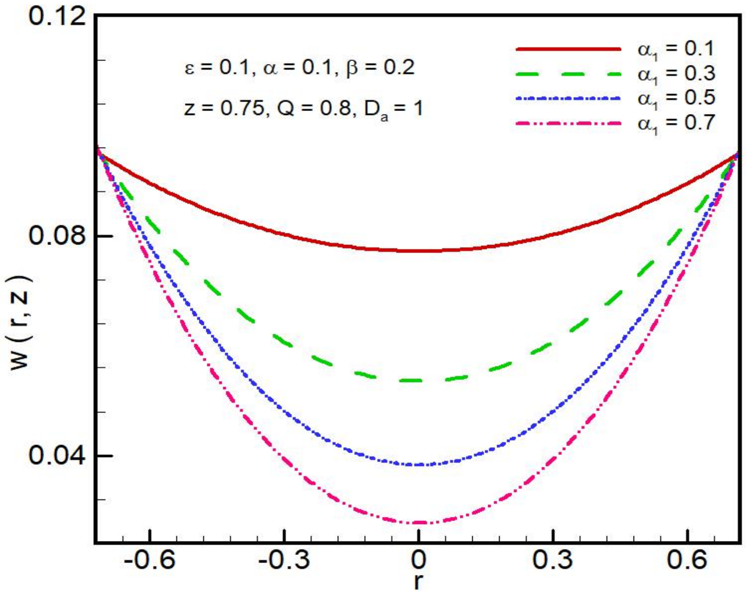

Fig. 2.2(a) Velocity Profile w(r, z) at $\alpha_1 = 0.1, 0.3, 0.5, 0.7.$

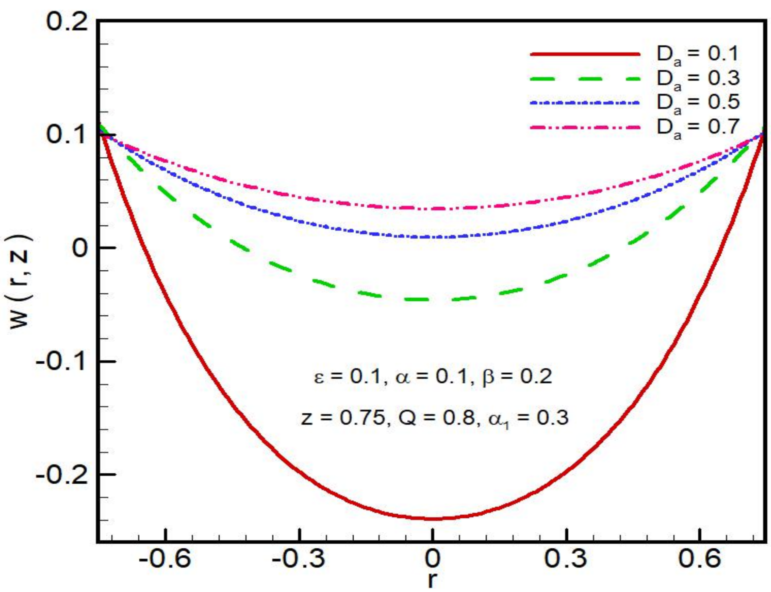

Fig. 2.2(b) Velocity Profile w(r, z) at $D_a = 0.1, 0.3, 0.5, 0.7.$

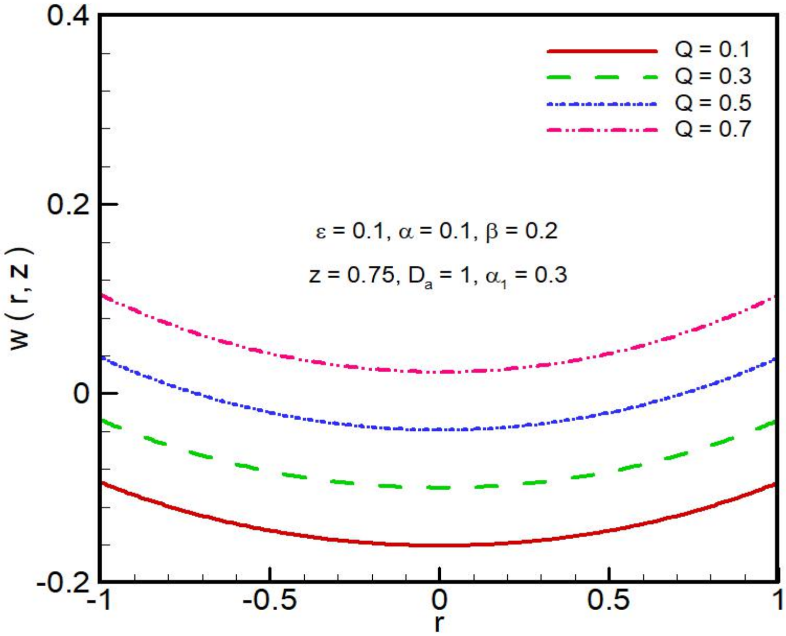

Fig. 2.2(c) Velocity Profile w(r, z) at $Q = 0.1, 0.3, 0.5, 0.7.$

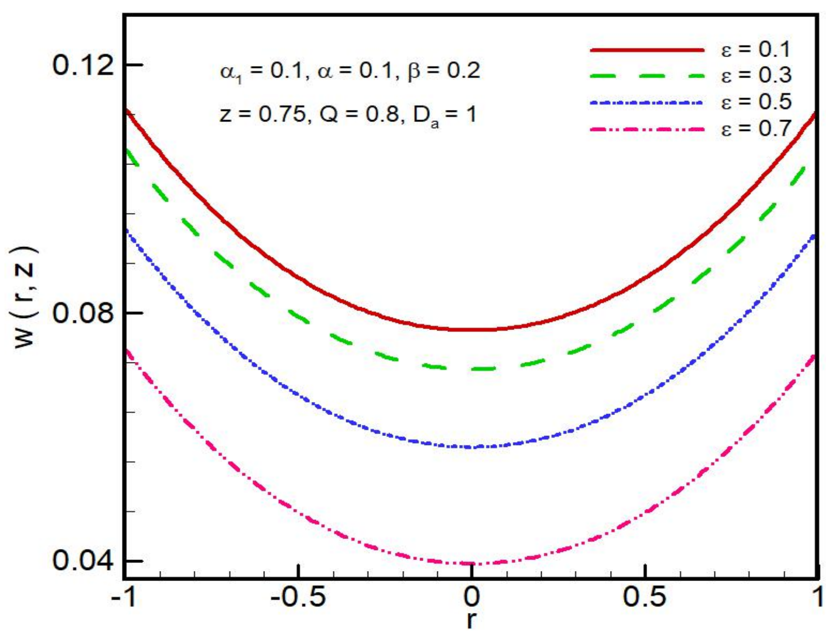

Fig. 2.2(d) Velocity Profile w(r, z) at $\varepsilon = 0.1, 0.3, 0.5, 0.7.$

Figures 2.2(a)-2.2(d) shows the graphs for velocity profile. It is clear from 2.2(a) that velocity decreases by increasing slip parameter α_1 and it gains magnitude by decreasing slip parameter. Fig. 2.2(b) depicts that velocity of fluid gains magnitude by increasing Darcy number and vice versa. It shows that the velocity rises as the permeability[7] of the medium rises and it decreases with decrease in permeability. Fig. 2.2(c) shows that as the flow rate Q gains magnitude then the velocity of fluid also rises and there is decrease in velocity by decreasing flow rate. Fig. 2.2(d) shows that the velocity decreases by rising cilia length and vice versa. All above graphs show that velocity has highest estimation at walls of tube and least at the centre. When $\varepsilon = 0$ then it means that cilia length parameter is zero which implies there is no metachronal wave. In such case, due to flexibility of walls, the flow is completely peristaltic and is therefore not considered here.

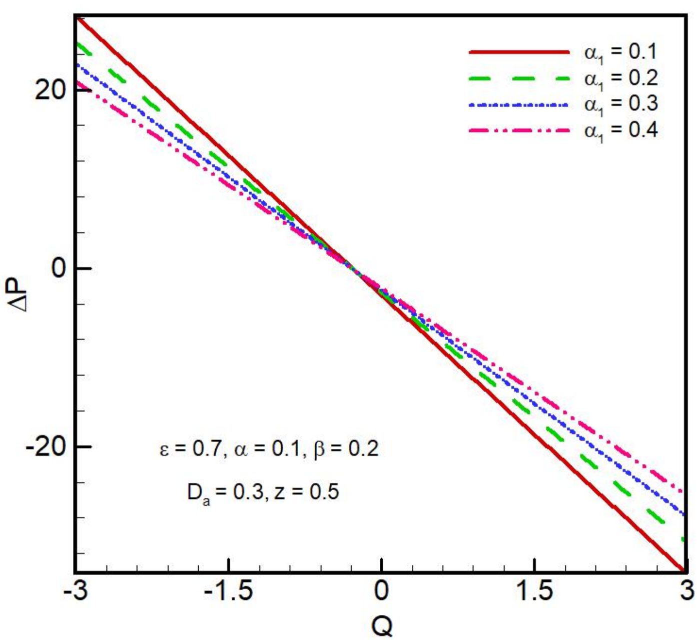

Fig. 2.3(a) Pressure rise vs. flow rate at $\alpha_1 = 0.1, 0.2, 0.3, 0.4.$

[7] Permeability is capacity of a porous medium that how much it allows the fluid to transmit through it.

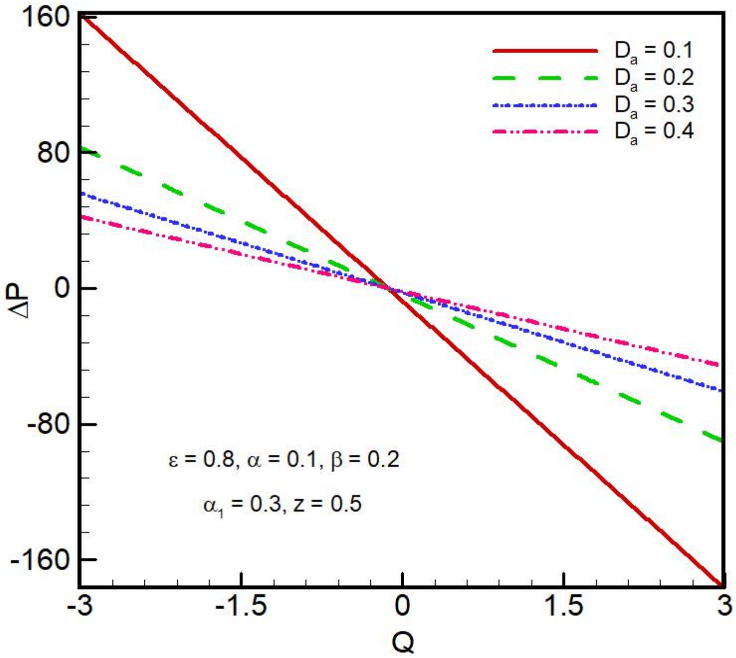

Fig. 2.3(b) Pressure rise vs. flow rate at $D_a = 0.1, 0.2, 0.3, 0.4.$

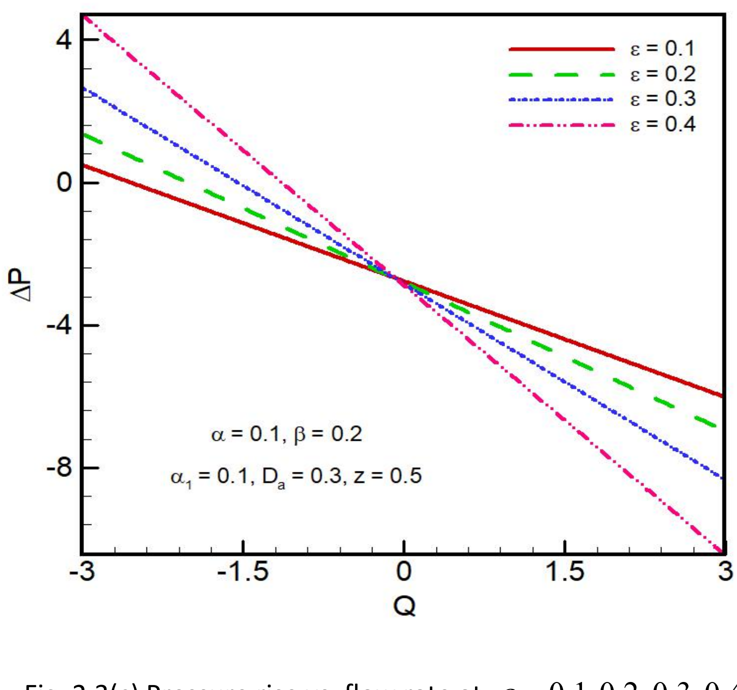

Fig. 2.3(c) Pressure rise vs. flow rate at $\varepsilon = 0.1, 0.2, 0.3, 0.4.$

In figures 2.3a-2.3c, pressure rise is plotted against the flow rate Q. These graphs depict a linear relation between these two. We have three different zones

(i) Push zone, in which $(\Delta P > 0)$,

(ii) free push zone, in which $(\Delta P = 0)$,

(iii) augmented push zone, in which $(\Delta P < 0)$.

Fig. 2.3(a) shows that pressure rise reduces as the slip parameter increments in pumping zone while it increases as slip parameter increases in augmented pumping zone. Fig. 2.3(b) depicts the same behaviour for Darcy number[8]. Fig. 2.3(c) shows that cilia length parameter has opposite behaviour than α_1 and ε.

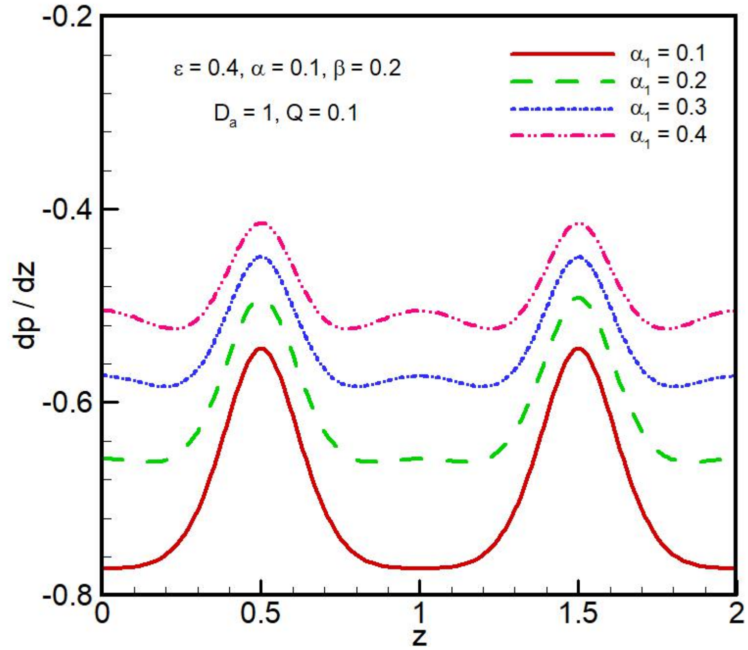

Fig. 2.4(a) Pressure gradient vs. Axial coordinate at $\alpha_1 = 0.1, 0.2, 0.3, 0.4.$

[8] Darcy number is a non-dimensional number and it is the ratio of medium's permeability and its area of cross-section.

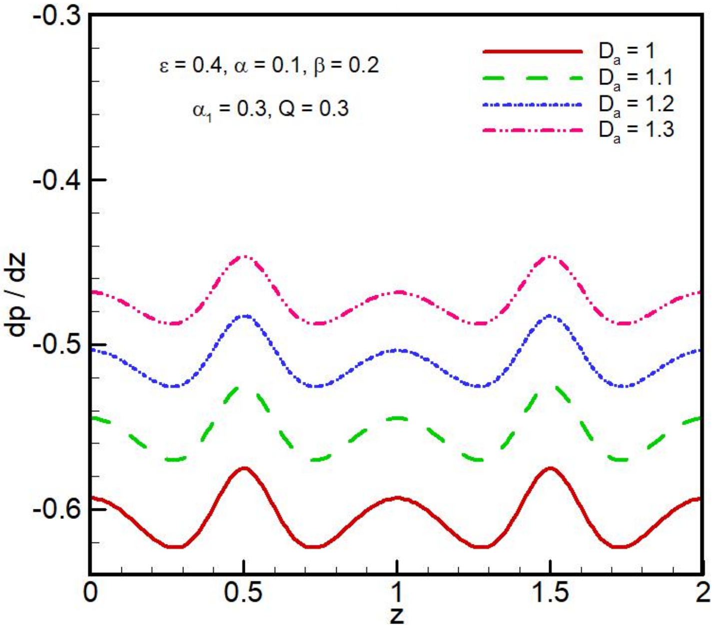

Fig. 2.4(b) Pressure gradient vs. Axial coordinate at $D_a = 1, 1.1, 1.2, 1.3$.

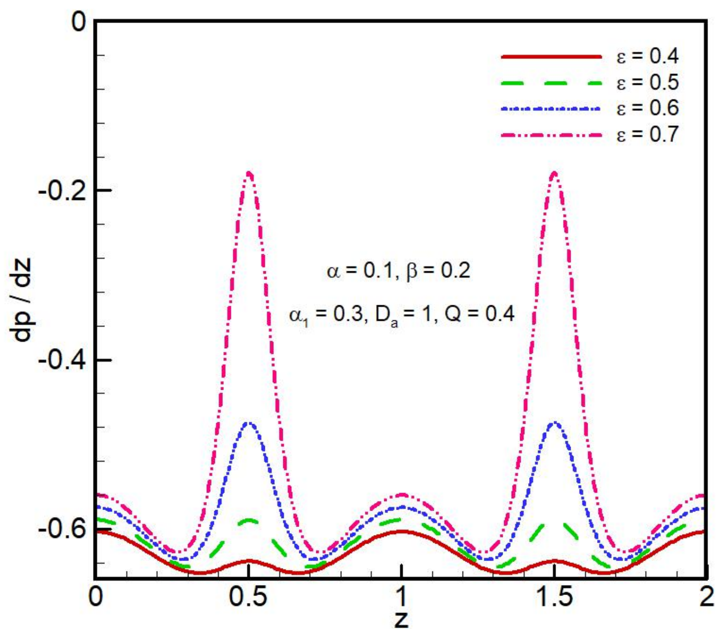

Fig. 2.4(c) Pressure gradient vs. Axial coordinate at $\varepsilon = 0.4, 0.5, 0.6, 0.7$.

Figures 2.4a-2.4c shows the pressure gradient plotted against axial coordinate z . The above graphs show that pressure gradient increases by increasing slip parameter α_1 , Darcy number D_a and also by increasing cilia length parameter ε . Pressure gradient increases rapidly by small change in cilia length parameter because when more cilia occur then fluid will take more pressure and it increases the pressure gradient.

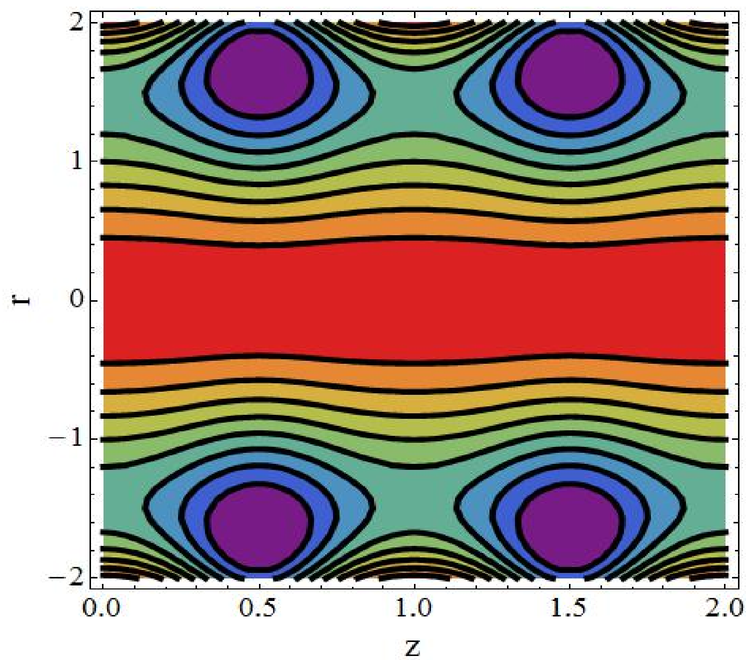

Fig. 2.5(a) Streamlines for the velocity profile at

$$\alpha_1 = 0.1, \varepsilon = 0.1, \alpha = 0.1, \beta = 0.2, D_a = 1, Q = 0.3.$$

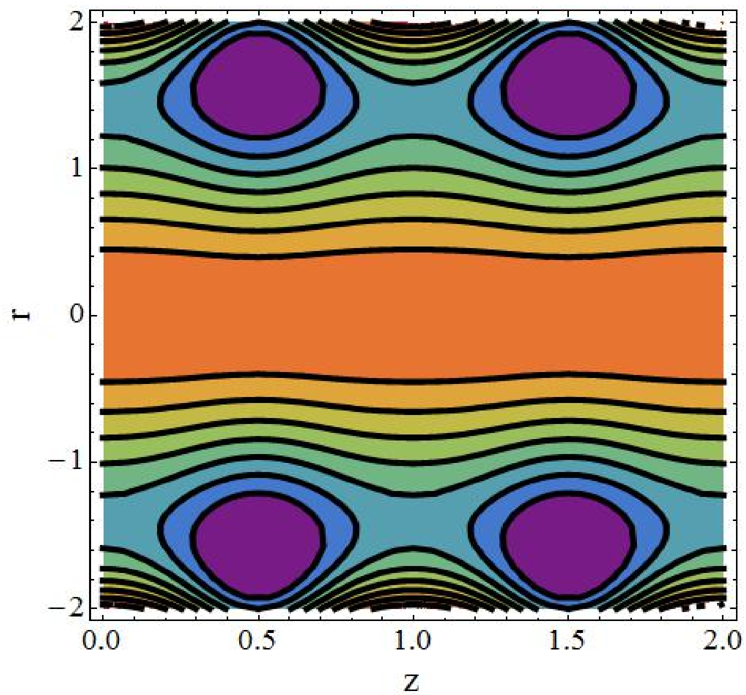

Fig. 2.5(b) Streamlines for the velocity profile at

$$\alpha_1 = 0.11, \varepsilon = 0.1, \alpha = 0.1, \beta = 0.2, D_a = 1, Q = 0.3.$$

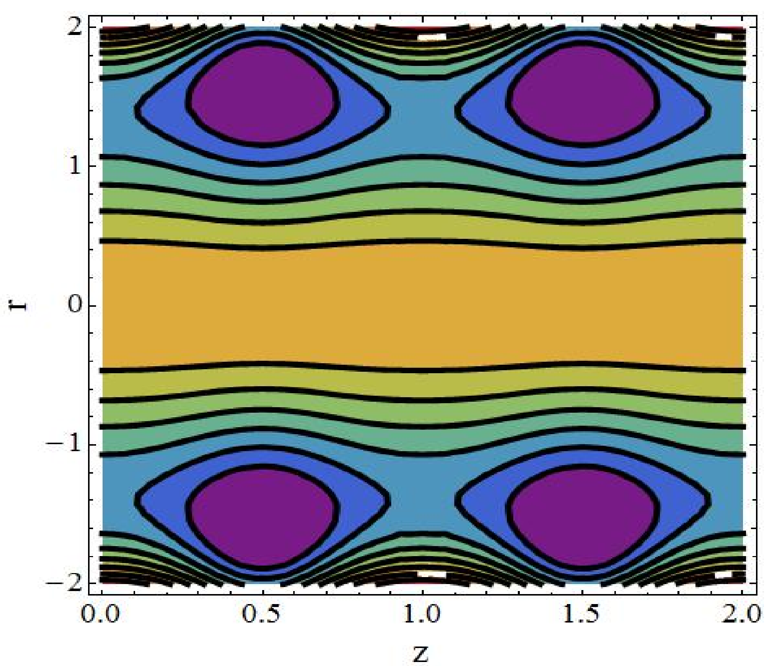

Fig. 2.5(c) Streamlines for the velocity profile at

$$\alpha_1 = 0.12, \varepsilon = 0.1, \alpha = 0.1, \beta = 0.2, D_a = 1, Q = 0.3.$$

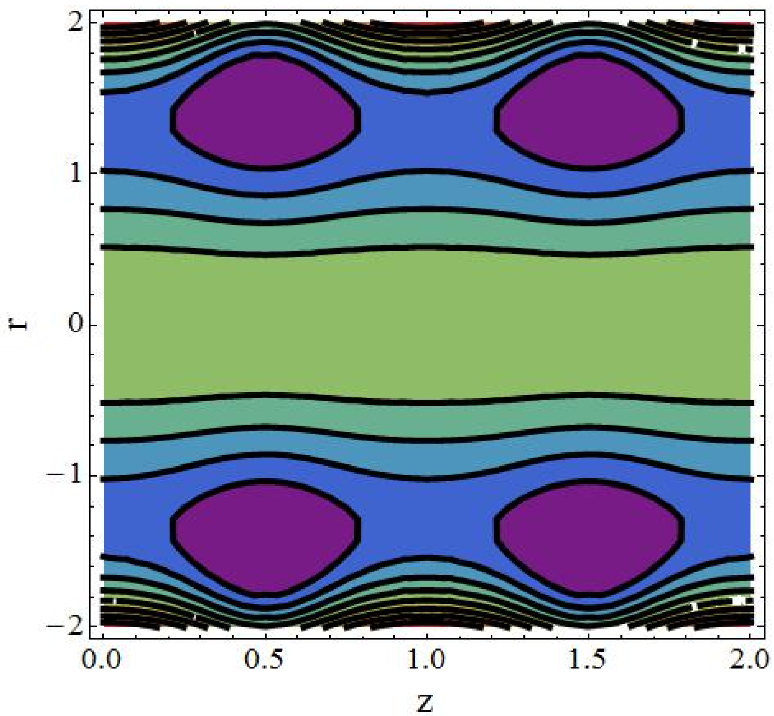

Fig. 2.5(d) Streamlines for the velocity profile at

$$\alpha_1 = 0.15, \varepsilon = 0.1, \alpha = 0.1, \beta = 0.2, D_a = 1, Q = 0.3.$$

Figures 2.5a-2.5d show streamlines for the velocity field. The above graphs depict that the trapping of bolus increases in size as the value of slip parameter increases. A peristaltic wave is produced by contraction of smooth muscle tissues in a sequence. Fluid moves easily at the centre of the tube and free stream arise at the centre. Therefore more trapping of bolus occurs near the walls.

Conclusions:

This research includes the study of creeping flow produced due to metachronal wave. The main reason behind this flow and production of metachronal waves is cilia beating. This examine is relevant to biomimetic propulsion mechanism that includes necessary medication by using artificial cilia. The present research will be helpful in more laboratory work. The significant points related to above research are describes as

1. Velocity of fluid gains magnitude by increasing Darcy number while it shows opposite behaviour for slip parameter.

2. Axial velocity increases with greater flow rate whereas it decreases with increasing axial coordinate.

3. In pumping region, by increasing slip velocity and permeability, the pressure rise decreases.

4. There is opposite effect of Axial coordinate and Darcy number on rise in pressure.

5. The trapping of bolus upturns by rising the value of slip parameter and it is maximum near the walls.

Chapter 3

Heat transfer analysis of MHD viscous fluid in a ciliated tube with entropy generation

3.1. Introduction:

This chapter includes the study of transfer of heat and entropy[9] generation of MHD[10] viscous fluid flowing through a ciliated tube. Heat transfer study has huge importance in various biomedical and biological industry problems. The metachronal wave propagation is main cause behind this creeping viscous flow. A low Reynolds number is used as the inertial forces are weaker than viscous forces and also creeping flow limitations are fulfilled. For cilia movement, a very large wavelength of metachronal wave is taken into account. The transfer of heat through the flow is examined by entropy generation. Numerical solutions are calculated by using mathematica. Exact mathematical solutions are calculated and analyzed with the help of graphs. Streamlines are also plotted.

---

[9] Entropy occurs due to disorder or randomness in a system.

[10] Magnetohydrodynamics (MHD) deals with electrically conducting fluids.

3.2. Mathematical formulation:

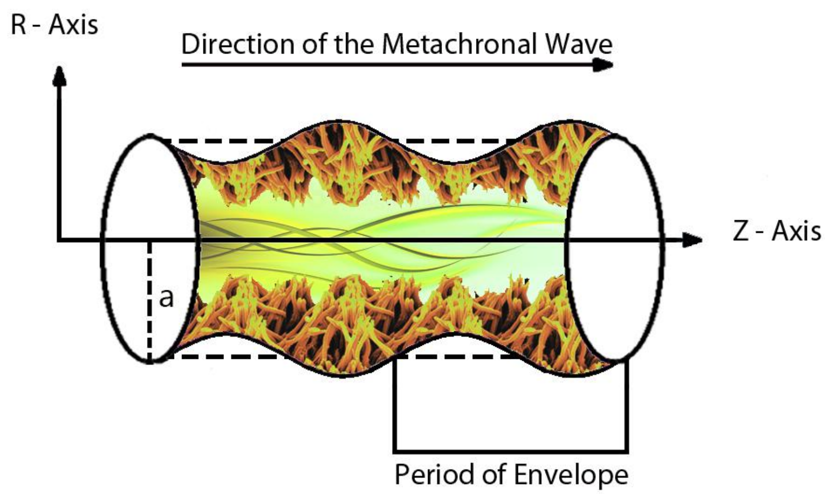

Figure 2 : Geometry of the problem

An incompressible Newtonian flow through a tube containing cilia is considered. Because of integrate beating of cilia metachronal waves are produced and there is no slip at the wall. The go with the flow is produced because of integrate beating of cilia. A cylindrical coordinate frame of reference $(\overline{R},\overline{Z})$ is selected so that $\overline{Z}$ -axis is oriented alongside the significant line of tube having $\overline{R}$ -axis normal to it. Cilia show wave movement with velocity, c, alongside the outer wall of tube. The envelope of cilia pointers are described mathematically as [1,9]

$$\overline{R}=\overline{H}=\bar{f}(\overline{Z},\bar{t})=a+a\varepsilon\cos\left(\frac{2\pi}{\lambda}(\overline{Z}-c\bar{t})\right),$$
$$\overline{Z}=\overline{g}(\overline{Z},\overline{Z}_0,\bar{t})=a+a\varepsilon\alpha\sin\left(\frac{2\pi}{\lambda}(\overline{Z}-c\bar{t})\right), \tag{1}$$

Here ε is cilia length parameter, a shows radius of tube, λ depicts wavelength, c shows pace of wave, α depicts eccentricity for elliptic movement and $\overline{Z}$ is the reference location of particle.

The velocities are given by

$$\overline{W}=\left(\frac{\partial\overline{Z}}{\partial\bar{t}}\right)_{\overline{Z}_0}=\frac{\partial\overline{g}}{\partial\bar{t}}+\frac{\partial\overline{g}}{\partial\overline{Z}}\frac{\partial\overline{Z}}{\partial\bar{t}}=\frac{\partial\overline{g}}{\partial\bar{t}}+\frac{\partial\overline{g}}{\partial\overline{Z}}\overline{W},$$

$$\overline{U}=\left(\frac{\partial\overline{R}}{\partial\bar{t}}\right)_{\overline{Z}_0}=\frac{\partial\bar{f}}{\partial\bar{t}}+\frac{\partial\bar{f}}{\partial\overline{Z}}\frac{\partial\overline{Z}}{\partial\bar{t}}=\frac{\partial\bar{f}}{\partial\bar{t}}+\frac{\partial\bar{f}}{\partial\overline{Z}}\overline{W}, \tag{2}$$

Using eq. (2) in (1), we have

$$\overline{W}=\frac{-(2\pi/\lambda)[\varepsilon\alpha ac\cos(2\pi/\lambda)(\overline{Z}-c\bar{t})]}{[1-(2\pi/\lambda)\{\varepsilon\alpha a\cos(2\pi/\lambda)(\overline{Z}-c\bar{t})\}]},$$

$$\overline{U}=\frac{(2\pi/\lambda)[\varepsilon ac\sin(2\pi/\lambda)(\overline{Z}-c\bar{t})]}{[1-(2\pi/\lambda)\{\varepsilon\alpha a\cos(2\pi/\lambda)(\overline{Z}-c\bar{t})\}]}, \tag{3}$$

This flow is transient for fixed frame $(\overline{R},\overline{Z})$, but it is regular in a moving frame $(\bar{r},\bar{z})$. In moving frame, the viscous flow is expressed by these equations

Continuity Equation:

$$\frac{1}{\overline{R}}\frac{\partial(\overline{R}\,\overline{U})}{\partial\overline{R}}+\frac{\partial\overline{W}}{\partial\overline{Z}}=0, \tag{4}$$

R-direction momentum equation:

$$\rho\left[\frac{\partial\overline{U}}{\partial\bar{t}}+\overline{U}\frac{\partial\overline{U}}{\partial\overline{R}}+\overline{W}\frac{\partial\overline{U}}{\partial\overline{Z}}\right]=-\frac{\partial\overline{P}}{\partial\overline{R}}+\mu\frac{\partial}{\partial\overline{R}}\left[2\frac{\partial\overline{U}}{\partial\overline{R}}\right]+\mu\frac{2}{\overline{R}}\left(\frac{\partial\overline{U}}{\partial\overline{R}}-\frac{\overline{U}}{\overline{R}}\right)+\mu\frac{\partial}{\partial\overline{Z}}\left(\frac{\partial\overline{U}}{\partial\overline{R}}+\frac{\partial\overline{W}}{\partial\overline{Z}}\right), \tag{5}$$

Z-direction momentum equation:

$$\rho\left[\frac{\partial\overline{W}}{\partial\bar{t}}+\overline{U}\frac{\partial\overline{W}}{\partial\overline{R}}+\overline{W}\frac{\partial\overline{W}}{\partial\overline{Z}}\right]=-\frac{\partial\overline{P}}{\partial\overline{Z}}+\mu\frac{\partial}{\partial\overline{Z}}\left[2\frac{\partial\overline{W}}{\partial\overline{Z}}\right]+\mu\frac{1}{\overline{R}}\frac{\partial}{\partial\overline{R}}\left[\overline{R}\left(\frac{\partial\overline{U}}{\partial\overline{Z}}+\frac{\partial\overline{W}}{\partial\overline{R}}\right)\right]-\sigma B_0^2\overline{W}, \tag{6}$$

Heat equation :

$$\frac{\partial \overline{T}}{\partial \overline{t}}+\rho_{cp}\left(\overline{U}\frac{\partial \overline{T}}{\partial \overline{R}}+\overline{W}\frac{\partial \overline{T}}{\partial \overline{Z}}\right)=\mu\left(2\left(\left(\frac{\partial \overline{U}}{\partial \overline{Z}}\right)^2+\left(\frac{\partial \overline{W}}{\partial \overline{R}}\right)^2\right)+\left(\frac{\partial \overline{U}}{\partial \overline{R}}+\frac{\partial \overline{W}}{\partial \overline{Z}}\right)^2\right)+k\left[\frac{\partial^2 \overline{T}}{\partial \overline{R}^2}+\frac{1}{\overline{R}}\frac{\partial \overline{T}}{\partial \overline{R}}+\frac{\partial^2 \overline{T}}{\partial \overline{Z}^2}\right], \quad (7)$$

where $\overline{T}$ is natural temperature of fluid, ρ_{cp} is heat capacitance, μ shows viscosity and k shows effective thermal conductivity.

The shift for the given frames are:

$$\overline{r}=\overline{R},\quad \overline{z}=\overline{Z}-c\overline{t},\quad \overline{u}=\overline{U},$$
$$\overline{w}=\overline{W}-c,\quad \overline{p}(\overline{z},\overline{r})=\overline{P}(\overline{Z},\overline{R},\overline{t}), \quad (8)$$

The given equations are transformed via the transformations :

$$\frac{1}{\overline{r}}\frac{\partial(\overline{r}\overline{u})}{\partial \overline{r}}+\frac{\partial \overline{w}}{\partial \overline{z}}=0, \quad (9)$$

$$\rho\left[\overline{u}\frac{\partial \overline{u}}{\partial \overline{r}}+\overline{w}\frac{\partial \overline{u}}{\partial \overline{z}}\right]=-\frac{\partial \overline{P}}{\partial \overline{r}}+\mu\frac{\partial}{\partial \overline{r}}\left[2\frac{\partial \overline{u}}{\partial \overline{r}}\right]+\mu\frac{2}{\overline{r}}\left(\frac{\partial \overline{u}}{\partial \overline{r}}-\frac{\overline{u}}{\overline{r}}\right)+\mu\frac{\partial}{\partial \overline{z}}\left[\left(\frac{\partial \overline{u}}{\partial \overline{r}}+\frac{\partial \overline{w}}{\partial \overline{z}}\right)\right], \quad (10)$$

$$\rho\left[\overline{u}\frac{\partial \overline{w}}{\partial \overline{r}}+\overline{w}\frac{\partial \overline{w}}{\partial \overline{z}}\right]=-\frac{\partial \overline{P}}{\partial \overline{z}}+\mu\frac{\partial}{\partial \overline{z}}\left[2\frac{\partial \overline{w}}{\partial \overline{z}}\right]+\mu\frac{1}{\overline{r}}\frac{\partial}{\partial \overline{r}}\left[\overline{r}\left(\frac{\partial \overline{u}}{\partial \overline{z}}+\frac{\partial \overline{w}}{\partial \overline{r}}\right)\right]-\sigma B_0^2(\overline{w}+c), \quad (11)$$

$$\frac{\partial \overline{T}}{\partial \overline{t}}+\rho_{cp}\left(\overline{u}\frac{\partial \overline{T}}{\partial \overline{r}}+\overline{w}\frac{\partial \overline{T}}{\partial \overline{z}}\right)=\mu\left(2\left(\left(\frac{\partial \overline{u}}{\partial \overline{z}}\right)^2+\left(\frac{\partial \overline{w}}{\partial \overline{r}}\right)^2\right)+\left(\frac{\partial \overline{u}}{\partial \overline{r}}+\frac{\partial \overline{w}}{\partial \overline{z}}\right)^2\right)+k\left[\frac{\partial^2 \overline{T}}{\partial \overline{r}^2}+\frac{1}{\overline{r}}\frac{\partial \overline{T}}{\partial \overline{r}}+\frac{\partial^2 \overline{T}}{\partial \overline{z}^2}\right], \quad (12)$$

Ellahi et al [42], Nadeem and Sadaf [46] have described the relevant boundary conditions.

$$\frac{\partial \overline{w}}{\partial \overline{r}}=0,\quad \text{at } r=0,$$
$$w=-1-\frac{2\pi\varepsilon\alpha\beta\cos(2\pi z)}{1-2\pi\varepsilon\alpha\beta\cos(2\pi z)},\quad \text{at } r=\overline{h}(z).$$
$$\frac{\partial \mathrm{T}}{\partial r}=0,\quad \text{at } \mathrm{r}=0,$$
$$\mathrm{T}=\mathrm{T}_0,\quad \text{at } r=\overline{h}(z). \quad (13)$$

Where $2\pi\varepsilon\alpha\beta\cos(2\pi z)/[1-2\pi\varepsilon\alpha\beta\cos(2\pi z)]$ is the cilia factor.

Now introducing the dimensionless variables

$$r=\frac{\bar{r}}{a},\ z=\frac{\bar{z}}{\lambda},\ w=\frac{\bar{w}}{c},\ u=\frac{\lambda\bar{u}}{ac},\ p=\frac{a^2\bar{p}}{c\lambda\mu},$$
$$\beta=\frac{a}{\lambda},\ M^2=\frac{\sigma B_0^2 R_0^2}{\mu},\ \theta=\frac{T-T_0}{T_0}. \tag{14}$$

Using above equations in equation 9 to 12, and applying estimations of enormous wavelength and low-set Reynolds number, then dimensionless equations are given by

$$\frac{\partial p}{\partial r}=0, \tag{15}$$
$$\frac{\mathrm{dp}}{\mathrm{dz}}=\frac{1}{r}\frac{\partial}{\partial r}\left(r\frac{\partial w}{\partial r}\right)-M^2(w+1), \tag{16}$$

$$\frac{1}{r}\frac{\partial}{\partial r}\left(r\frac{\partial\theta}{\partial r}\right)+B_r\left(\frac{\partial w}{\partial r}\right)^2=0, \tag{17}$$

The non-dimensional conditions on boundaries are

$$\frac{\partial w}{\partial r}=0,\qquad at\ \ r=0, \tag{16a}$$
$$w=-1-\frac{2\pi\varepsilon\alpha\beta\cos(2\pi z)}{1-2\pi\varepsilon\alpha\beta\cos(2\pi z)},$$
$$at\ \ r=h(z)=1+\varepsilon\cos(2\pi z). \tag{16b}$$

And

$$\frac{\partial\theta}{\partial r}=0,\qquad \text{at}\quad r=0, \tag{17a}$$
$$\theta=0,\qquad \text{at}\ \ r=h(z)=1+\varepsilon\cos(2\pi z). \tag{17b}$$

3.3. Viscous dissipation and entropy generation analysis

These equations [27-37], the dimensional viscous dissipation[11] term $\overline{\Phi}_1$ is defined as

$$\overline{\Phi}_1 = \mu\left[2\left(\left(\frac{\partial \overline{u}}{\partial \overline{z}}\right)^2 + \left(\frac{\partial \overline{w}}{\partial \overline{r}}\right)^2\right) + \left(\frac{\partial \overline{u}}{\partial \overline{r}} + \frac{\partial \overline{w}}{\partial \overline{z}}\right)^2\right], \tag{18}$$

Also the entropy generation with dimensions has been described by [27-37]

$$S'''_{gen} = \frac{k}{\overline{\theta}_0^2}\left[\left(\frac{\partial \overline{T}}{\partial \overline{r}}\right)^2 + \left(\frac{\partial \overline{T}}{\partial \overline{z}}\right)^2\right] + \frac{\overline{\Phi}_1}{\overline{\theta}_0}, \tag{19}$$

Entropy generation in non-dimensional pattern has been calculated by

$$N_s = \frac{S'''_{gen}}{S'''_G} = \left(\frac{\partial \theta}{\partial r}\right)^2 + \theta_0 B_r \left(\frac{\partial w}{\partial r}\right)^2, \tag{20}$$

Where

$$S'''_G = \frac{k\overline{T}_0^2}{\overline{\theta}_0^2 a^2}, \quad B_r = \frac{c^2\mu}{k\overline{T}_0}, \quad \theta_0 = \frac{\overline{\theta}_0}{\overline{T}_0}. \tag{21}$$

Entropy in equation (20) comprises of two parts. First one is because of measurable temperature dissimilarity and the later is because of viscous effects. Now Bejan number is determined as [27-37].

$$Be = \frac{Ns_{cond}}{Ns_{cond} + Ns_{visc}}, \tag{22}$$

3.4. Exact Solution:

Now by solving Eqs. 15 and 16, and applying relevant boundary conditions $(16, a, b)$, we have the velocity

---

[11] Viscous dissipation is defined as an irreversible process in which the work that is done by a fluid on neighbouring layers is transformed into heat.

$$w(r,z) = -1 - \frac{1}{M^2}\frac{dp}{dz} + \frac{\left[2\pi\varepsilon\alpha\beta\cos(2\pi\, z)\left(\frac{dp}{dz} + M^2\right) - \frac{dp}{dz}\right] I_0(Mr)}{M^2(2\pi\varepsilon\alpha\beta\cos(2\pi\, z) - 1) I_o(hM)}. \tag{23}$$

The volume flow rate is calculated by

$$F = 2\pi \int_0^h rwdr. \tag{24}$$

Now we integrate the above expression for flow rate and have

$$\frac{dp}{dz} = \frac{M^2\left[MI_0(hM)\left((1-2\pi\varepsilon\alpha\beta\cos(2\pi\, z))(F+h^2\pi)\right) + 4h\pi^2\varepsilon\alpha\beta\cos(2\pi\, z)I_1(hM)\right]}{h\pi(-1+2\pi\varepsilon\alpha\beta\cos(2\pi\, z))(hMI_0(hM) - 2I_1(hM))}. \tag{25}$$

The flow rates are linked in two frames as:

$$Q = F + \frac{1}{2}\left(1 + \frac{\varepsilon^2}{2}\right), \tag{26}$$

The rise in pressure (ΔP) is calculated by:

$$\Delta P = \int_0^1 \frac{dp}{dz} dz. \tag{27}$$

Now put Eq. (23) in Eq. (17) , we have temperature profile

$$\theta(r,z) = \frac{-B_r\left(-\frac{dp}{dz} + \left(M^2 + \frac{dp}{dz}\right)(2\pi\varepsilon\alpha\beta\cos(2\pi\, z))\right)^2 \left[\begin{array}{l} I_0(hM)^2(-1+h^2M^2) + I_0(Mr)^2(1-M^2r^2) \\ + M\left(rI_0(Mr)I_1(Mr) - hI_0(hM)I_1(hM)\right) \\ + M^2\left(r^2I_1(Mr)^2 - h^2I_1(hM)^2\right) \end{array}\right]}{2M^4\left(-1+2\pi\varepsilon\alpha\beta\cos(2\pi\, z)\right)^2 I_0(hM)^2}, \tag{28}$$

3.5. Results and discussion:

This segment describes the graphical illustration of velocity field, temperature profile, entropy generation Ns, bejan number[12] B_e, pressure gradient and streamlines for different physical constraints . The graphs for velocity field $w(r,z)$ are shown in Figs. 3.2(a)-3.2(c).

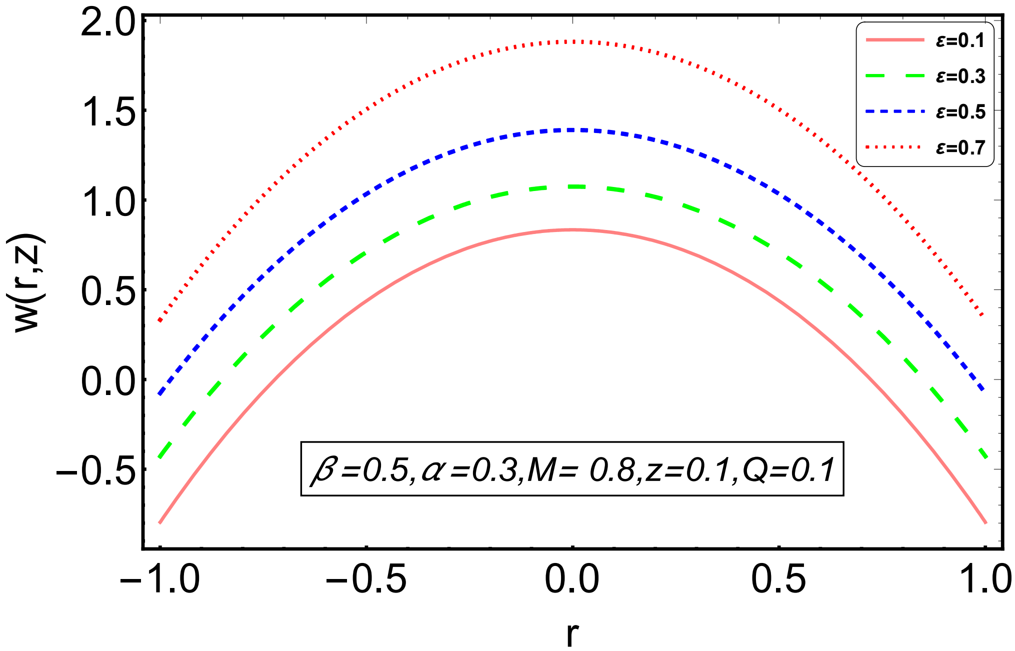

Fig. 3.2(a). Velocity profile w(r,z) at $\varepsilon = 0.1, 0.3, 0.5, 0.7$.

[12] Bejan number is non-dimensional drop in pressure through a channel of finite length. It is the ratio of irreversibility of heat transfer to absolute irreversibility because of both transfer of heat and viscosity.

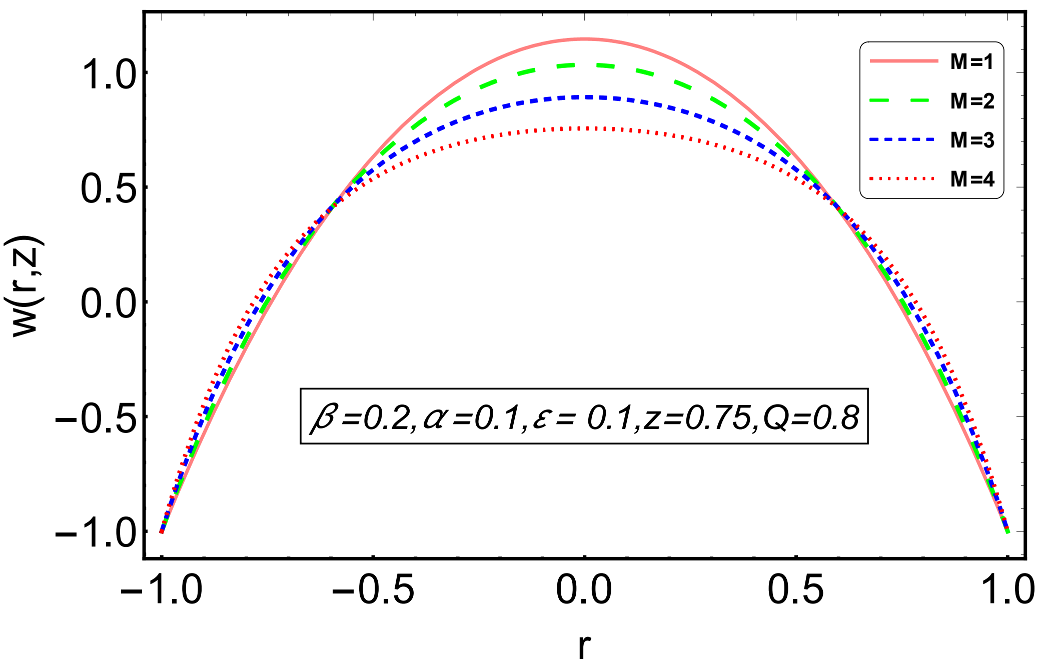

Fig.3.2(b) Velocity profile w(r,z) at M=1,2,3,4.

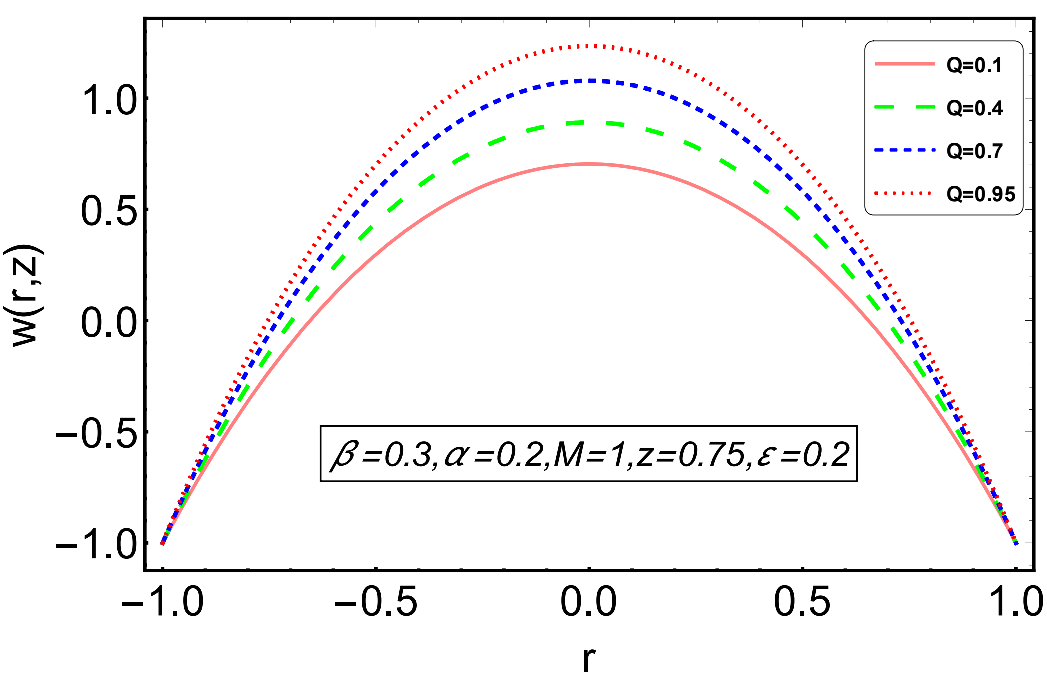

Fig.3.2(c) Velocity profile w(r,z) at Q=0.1,0.4,0.7,0.95.

Figures 3.2a-3.2c show the parabolic nature of the velocity profile. Figure 2a shows that , by increasing cilia length parameter (ε) , the velocity gains magnitude. The special case of $\varepsilon = 0$ implies the absence of metachronal wave by vanishing cilia. In such case, due to flexibility of walls, the flow is completely peristaltic and is therefore not considered here. Figure 2b shows that when the Hartmann number[13] M rises then velocity diminishes and vice versa. Figure 2c shows effect of flow rate Q on velocity of fluid and by increasing the flow rate, velocity of fluid also increases. Therefore, Propulsion is directly proportional to flow rates.

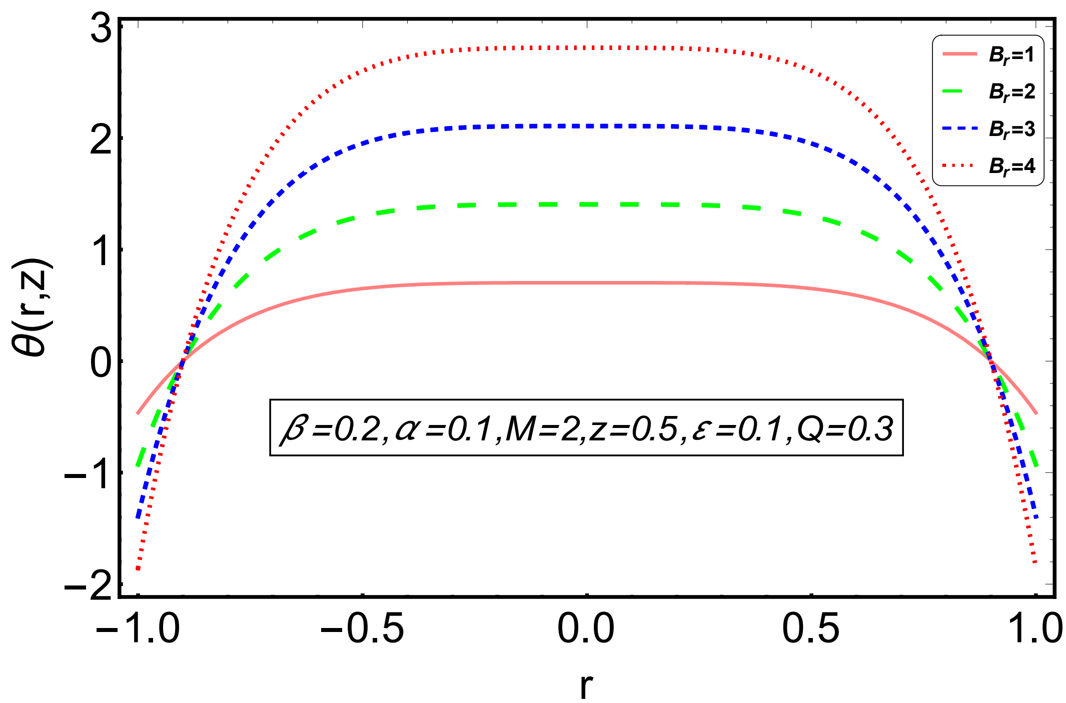

Fig.3.3(a) Temperature Profile $\theta(r,z)$ at $B_r = 1,2,3,4$.

[13] Hartmann number is non-dimensional number and it is ratio of the electromagnetic forces and the viscous forces.

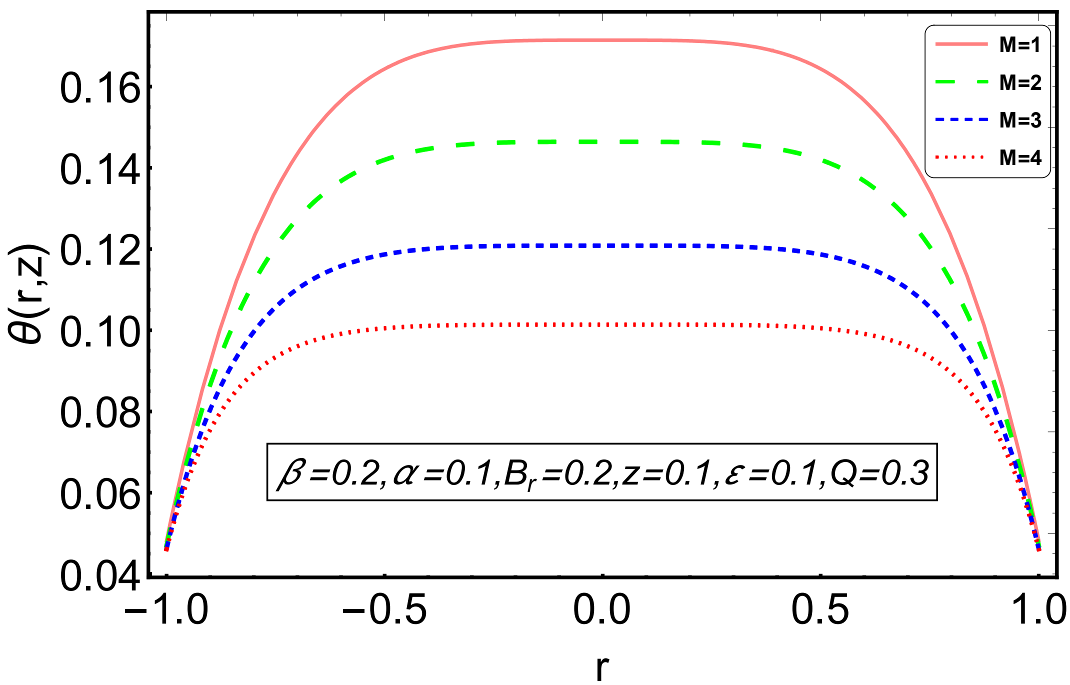

Fig.3.3(b) Temperature Profile $\theta(r,z)$ at M=1,2,3,4.

Figures 3.3a-3.3b show the behaviour of temperature in the tube. Temperature gains its highest estimation at centre and lowest estimation at boundaries of tube. Temperature rises as the Brinkman number[14] B_r is increased but decreases as the Hartmann number M is increased. which analyze that as Hartmann number is ratio of the electromagnetic forces and the viscous force so when electromagnetic force are greater than viscous forces then temperature reduces.

[14] Brickmann number is dimensionless number defined as ratio of heat generated due to viscous dissipation and heat transferred because of conduction of molecules.

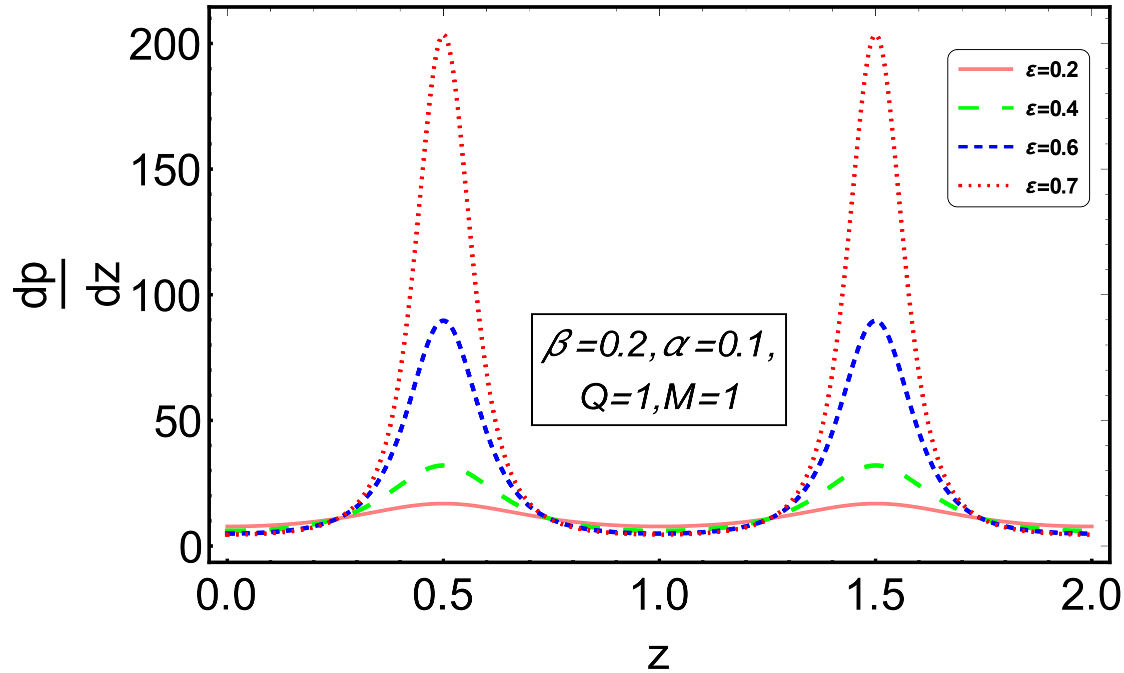

Fig.3.4(a) Pressure gradient vs. Axial coordinate at $\varepsilon = 0.2, 0.4, 0.6, 0.7$.

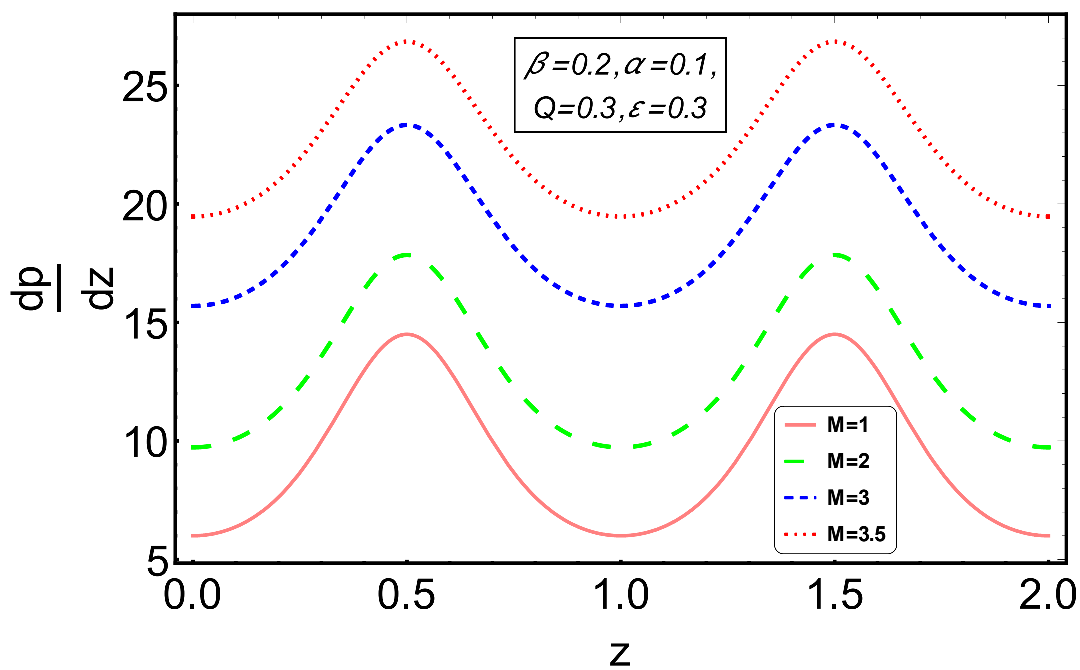

Fig.3.4(b) Pressure gradient vs. axial coordinate at $M = 1, 2, 3, 3.5$.

Figures 3.4a-3.4b show the pressure gradient distribution with axial coordinate. Fig. 4(a) depicts that the pressure gradient increases by small change in cilia length ε because when more cilia occurs then fluid will take more pressure and move that increases the pressure gradient .Pressure gradient also increases by increasing Hartmann number M ,see Fig.3.4(b). This rise in pressure gradient is because of the rise in electromagnetic forces.

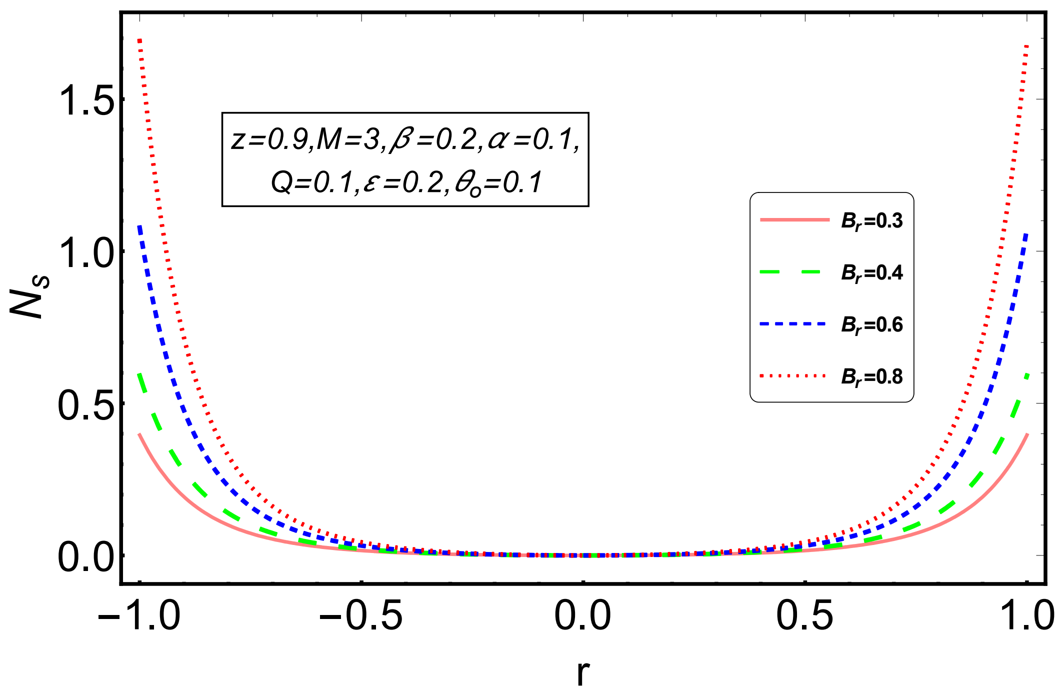

Fig.3.5(a) Entropy generation number $N_s(r,z)$ at $B_r = 0.3,0.4,0.6,0.8.$

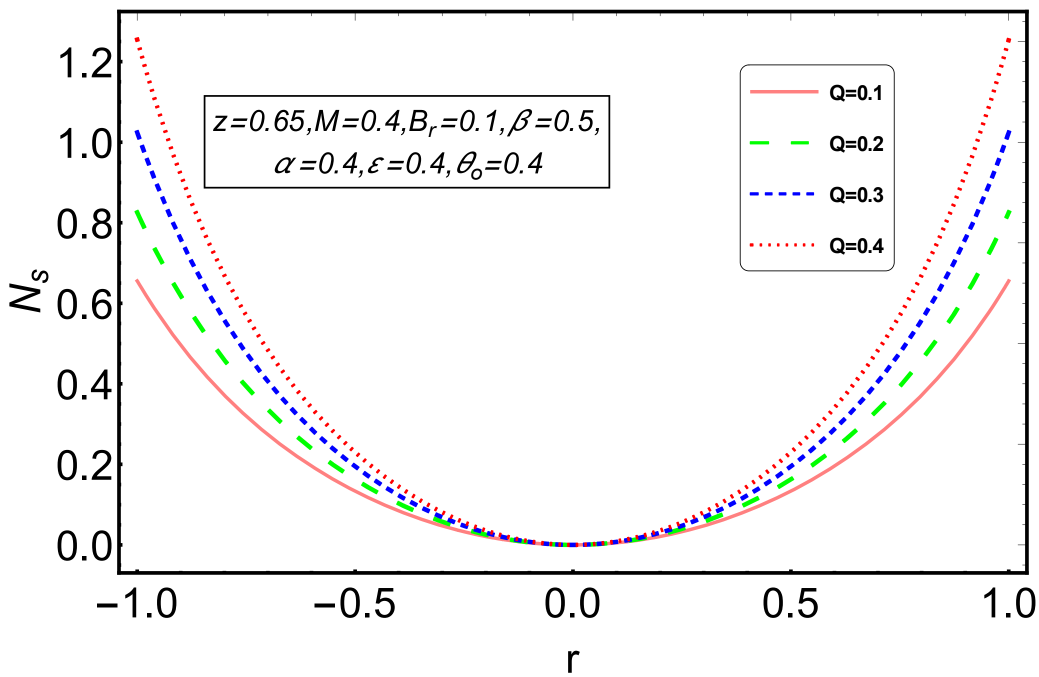

Fig.3.5(b) Entropy generation number $N_s(r,z)$ at Q=0.1,0.2,0.3,0.4.

In general, Entropy has a non-uniform behaviour. These figures 3.5(a), 3.5(b) show that entropy generation increases as the rate of flow Q and Brickmann number B_r increases and vice versa. By increasing the rate of flow Q and Brickmann number B_r , entropy generation grows at the walls. As entropy occurs because of disorder or randomness in system and since flow is uniform at the centre of tube so stationary behaviour occurs at the centre of the tube.

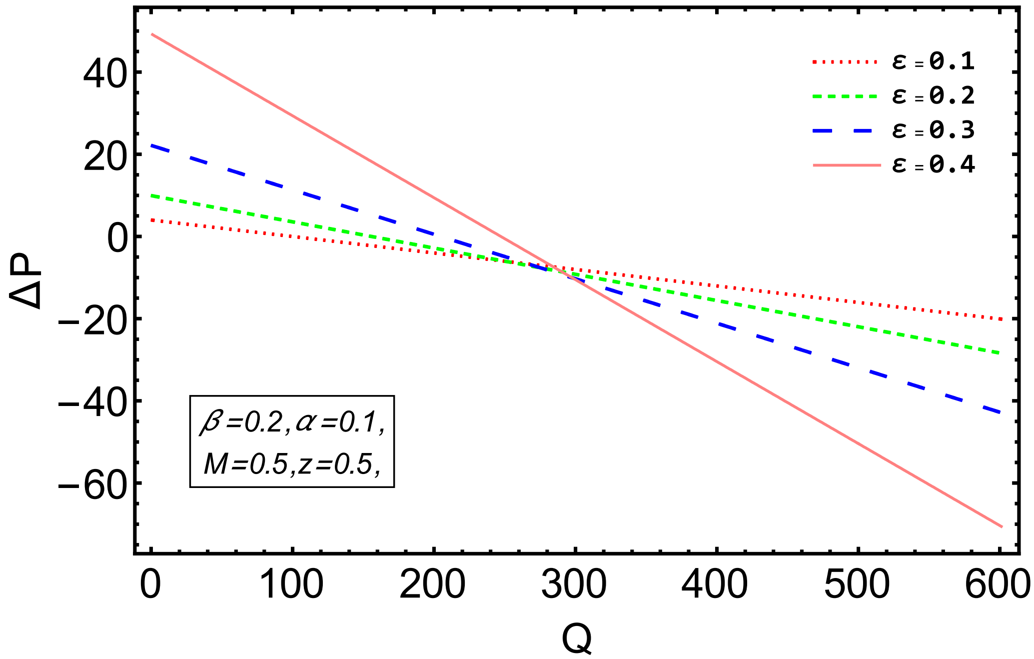

Fig.3.6(a) Pressure rise vs. flow rate at $\varepsilon = 0.1, 0.2, 0.3, 0.4$.

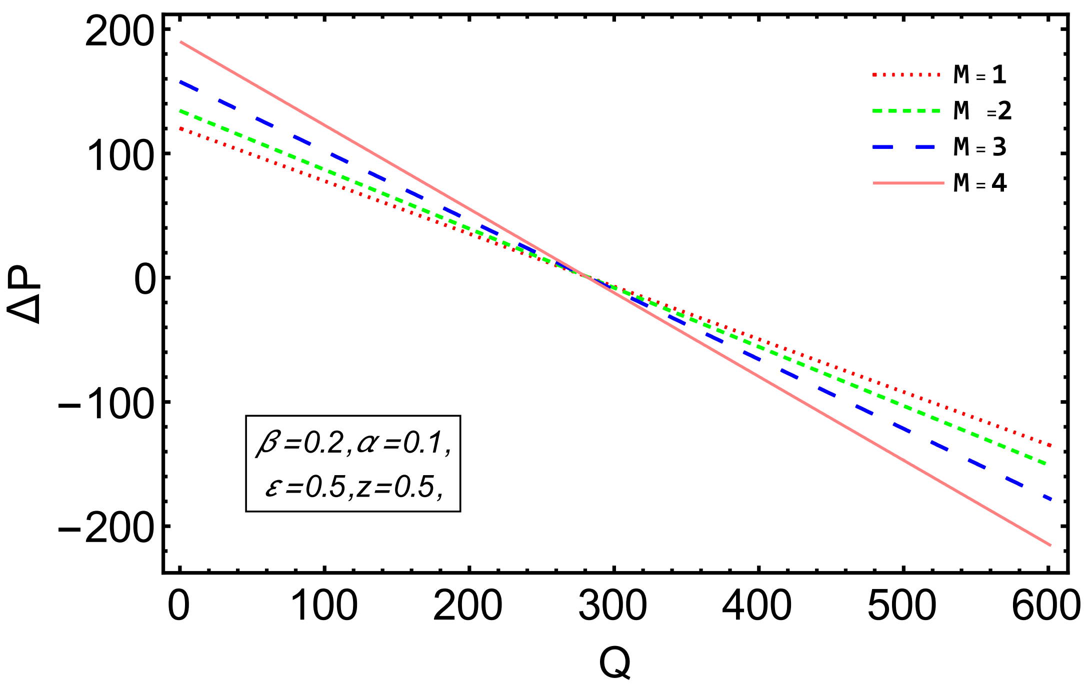

Fig.3.6(b) Pressure rise vs. flow rate at $M = 1,2,3,4$.

Figures 3.6a-3.6b show that pressure and the flow rate have linear relation. We have three different pumping zones:

(i) Push zone, for which $(\Delta P > 0)$,

(ii) Free push zone, for which $(\Delta P = 0)$,

(iii) Augmented push zone ,for which $(\Delta P < 0)$,

From figure 3.6a, In the pumping zone, increase in pressure is rising function of cilia length while in augmented pumping area, it is decreasing function. Pumping occurs from $0 \le Q \le 300$, while the Augmented pumping occurs in the region $301 \le Q \le 600$.

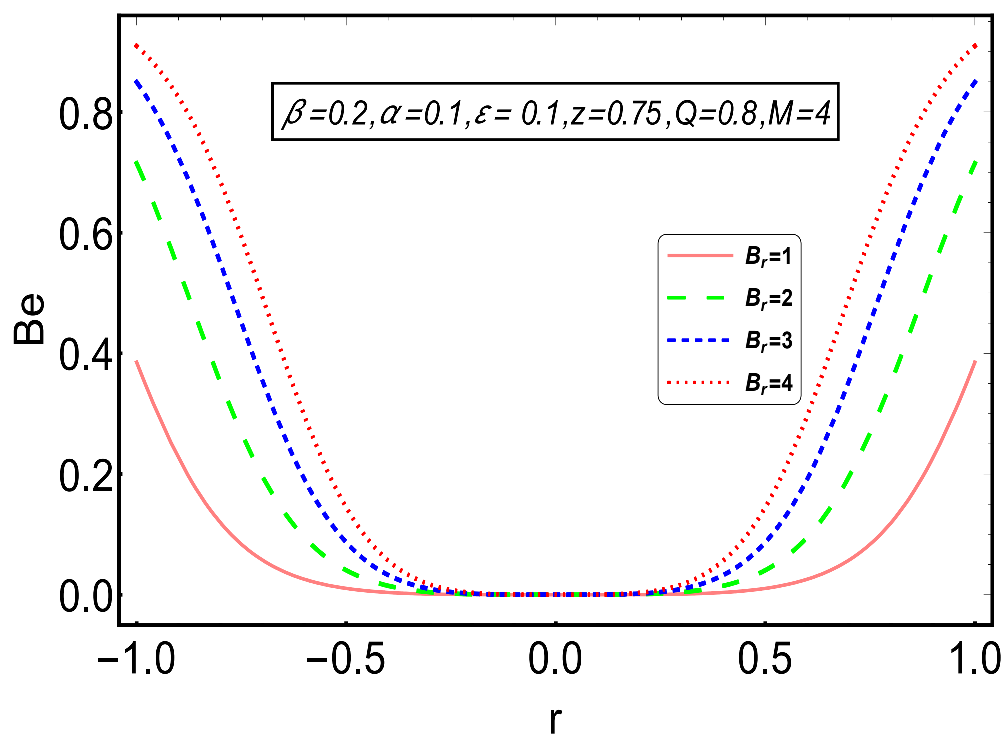

Fig. 3.7(a) Bejan number Be at $B_r = 1,2,3,4$.

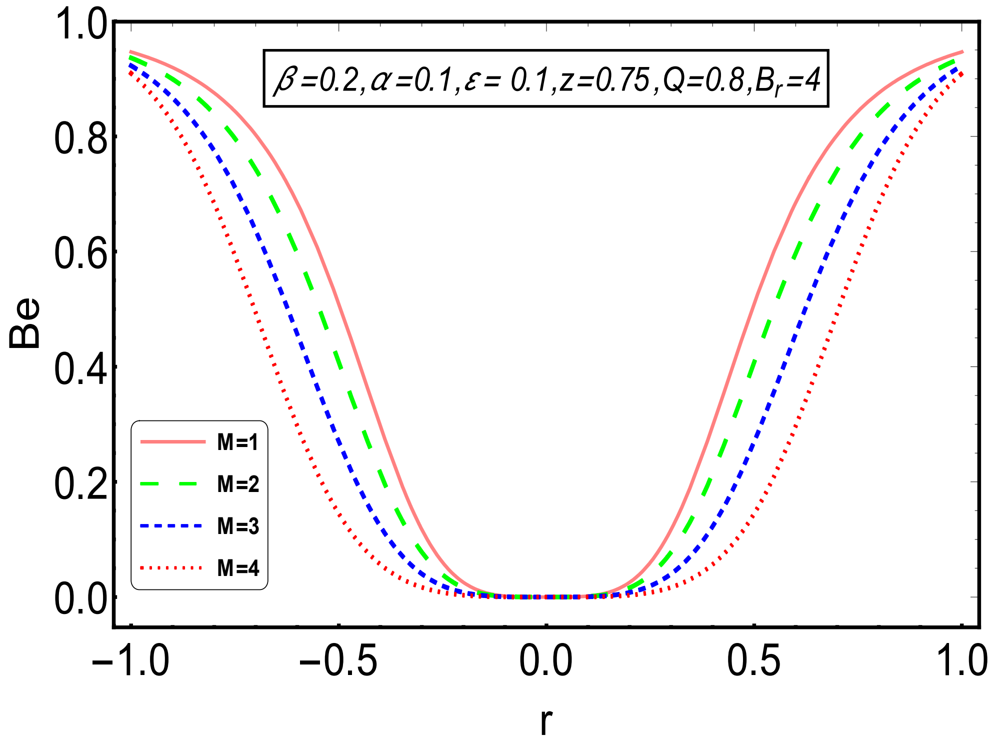

Fig. 3.7(b) Bejan number Be at M=1,2,3,4.

Figures 3.7(a), 3.7(b) depicts the behaviour of bejan number for various parameters. It is clear from 3.7(a) that bejan number varies directly with B_r . Further, 3.7(b) shows that bejan number varies inversely with Hartmann number M. Bejan number increases at walls and it has stationary behaviour at the centre of tube. Since bejan number depends on resistive forces so it is maximum near the walls as the resistive forces are higher near the walls whereas bejan number is minimum at the centre because resistance is minimum at the centre of the tube.

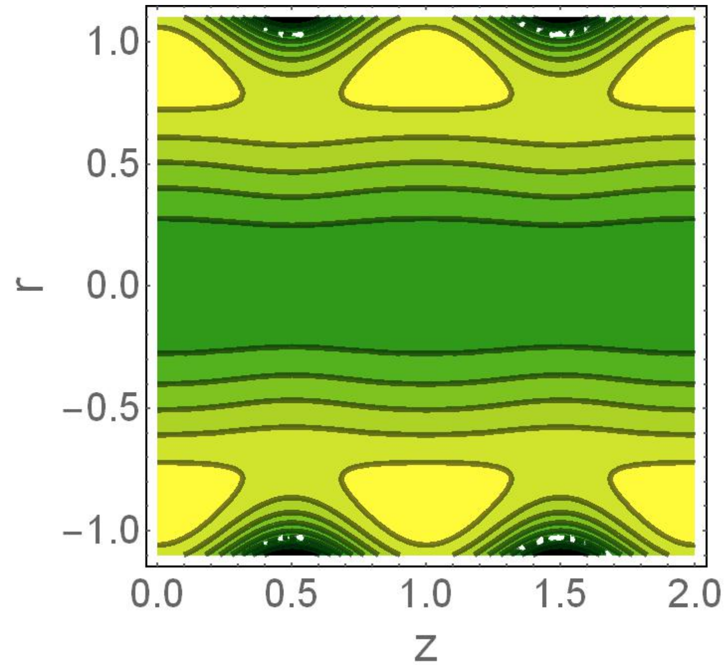

Fig. 3.8(a) Streamlines for velocity profile at

$\varepsilon = 0.122, M = 1.5, \alpha = 0.4, \beta = 0.1, Q = 2.$

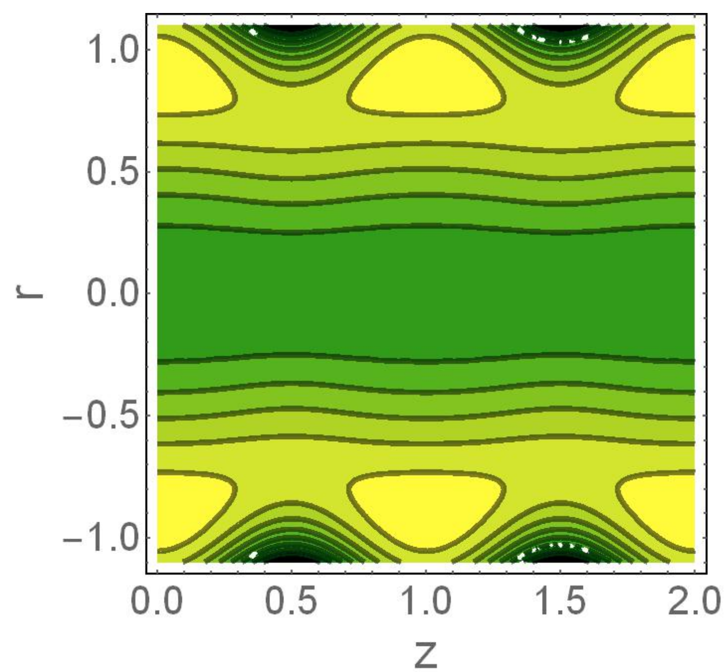

Fig. 3.8(b) Streamlines for velocity profile at

$\varepsilon = 0.124, M = 1.5, \alpha = 0.4, \beta = 0.1, Q = 2.$

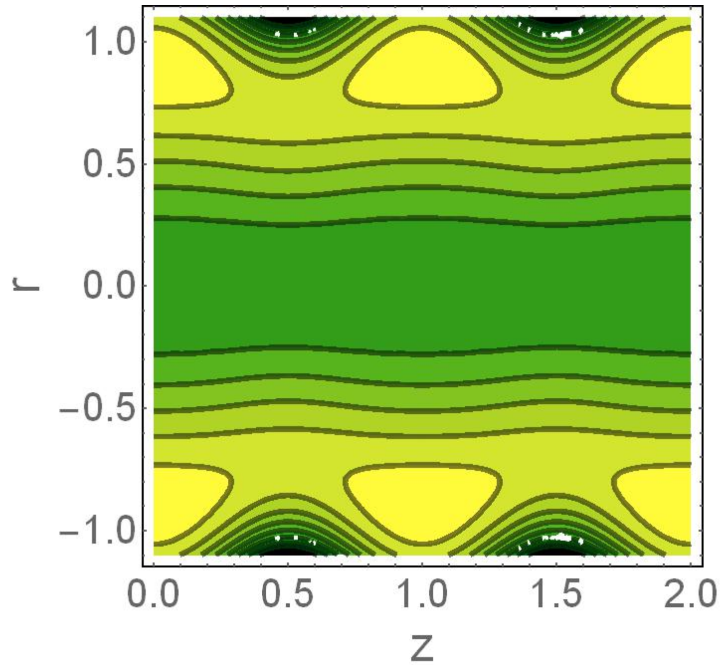

Fig. 3.8(c) Streamlines for the velocity profile at

$$\varepsilon = 0.125, M = 1.5, \alpha = 0.4, \beta = 0.1, Q = 2.$$

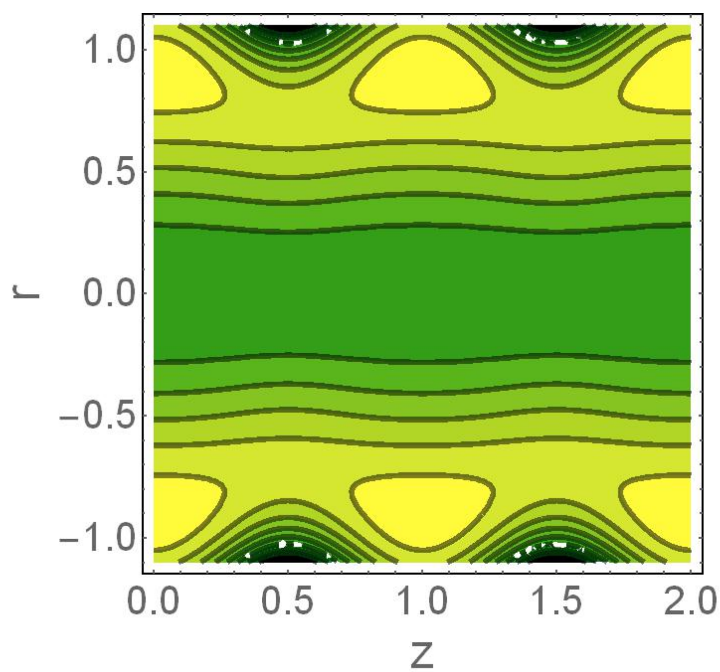

Fig. 3.8(d) Streamlines for the velocity profile at

$$\varepsilon = 0.127, M = 1.5, \alpha = 0.4, \beta = 0.1, Q = 2.$$

Conclusions:

This research includes the study of transfer of heat and entropy generation of MHD viscous fluid in a ciliated tube. The biological propulsion mechanisms, i.e. the role of movement of cilia tips in human respiration and also in urodynamics is the motivation behind this work. This study will further encourage the much wished scientific research. The significant deductions obtained from this study are

(i) If we increase Hartmann number then velocity decreases but it gains magnitude if flow rate is increased.

(ii) Axial velocity increases with greater flow rate whereas it decreases with increasing axial coordinate.

(iii) Temperature gains magnitude with an increase in Brickmann number B_r whereas it decreases by increasing Hartmann number M.

(iv) In the pumping zone, rise in pressure varies directly with cilia length parameter while in augmented pumping zone, pressure rise varies inversely with cilia length parameter.

(v) Entropy generation varies directly with flow rate Q and Brickmann number B_r. It increases near walls and it is stationary at centre because of uniform fluid flow at centre of tube.

(vi) The trapped bolus decreases in size by increasing cilia length parameter. Since the velocity of the fluid increases by increasing cilia length parameter and also pressure gradient increases.

References:

1. T Y Wu, On the theoretical modelling of aquatic and aerial animal locomotion, Adv. Appl. Mech. 38, 291 (2001)
2. T Y Wu, Reflections for resolution to some recent studies on fluid mechanics, in: Advances in engineering mechanics - Reflections and outlooks (World scientific, Singapore, 2006)
3. J Feng and S K Cho, Mini and Micro propulsion for medical swimmers, Micromachines 5, 97 (2014)
4. Ye Wang, Yang Gao and Hans M Wyss, Artificial cilia fabricated using magnetic fiber drawing generate substantial fluid flow, Microfluid Nanofluid 18, 167 (2015)
5. M A Sleigh, The biology of cilia and flagella (MacMillan, New York, USA, 1962)
6. T J Lardner and W J Shack, Cilia transport, Bull. Math. Biophys. 34, 25 (1972)
7. J R Blake, A model for the micro-structure in ciliated organisms, J. Fluid Mech, 55, 1 (1972)
8. T Y Wu, Fluid Mechanics of ciliary propulsion, Proc. Tenth Annual meeting of the Society of Engineering Science (Yale University, Connecticut, USA, 1973)
9. C Brennen, An oscillating-boundary-layer therory for ciliary propulsion, J. Fluid Mech. 65, 799 (1974)
10. M A Sleigh and E Aiello, The movement of water by cilia, Acta. Protozool. 11, 265 (1972)
11. H Agarwal and A Uddin, Cilia transport of bio-fluid with variable viscosity, Indian J. Pure Appl. Math. 15, 1128 (1984)
12. J R Blake, A spherical envelope approach to ciliary propulsion, J. Fluid Mech. 46, 199 (1971)
13. C E Miller, An investigation of the movement of Newtonian liquids initiated and sustained by the oscillation of mechanical cilia, Aspen Emphysema Conf. (Aspen, Colorado, USA, 1967)
14. C Barton and S Raynor, Analytical investigation of cilia induced mucous flow, Bull. Math. Biophys. 29, 419 (1967)
15. D J Smith, E A Gaffney and J R Blake, A viscoelastic traction layer model of muco-ciliary transport, Bull. Math. Biol. 69, 289 (2007)

16. A Dauptain, J Favier and A Battaro, Hydrodynamics of ciliary propulsion, J. Fluid Struct. 24, 1156 (2008)
17. S N Khaderi and P R Onck, Fluid structure interaction of three-dimensional magnetic artificial cilia, J. Fluid Mech. 708, 303 (2012)
18. S N Khaderi, J M J den Toonder and P R Onck, Fluid flow due to collective non-reciprocal motion of symmetrically-beating artificial cilia, Biomicrofluidics 6, 014106 (2012)
19. S N Khaderi, C B Craus, J Hussong, N Schorr, D J Belardi, J Westerweel, O Prucker, D J Ruhe, J M J den Toondere and P R Onck, Magnetically-actuated artificial cilia for microfluidic propulsion , Lab Chip 11, 2002 (2011)
20. G A Truskey, F Yuan and D F Katz, Transport phenomena in biological systems (Pearson, New Jersey, 2004)
21. O Coussy, Mechanics of porous continua (Butterworths, USA, 1993)
22. A R A Khaled and K Vafai, The role of porous media in modelling flow and heat transfer in biological tissues , Int. J. Heat Mass transfer 46, 4989 (2003)
23. P G Staffman, On the boundary condition at the surface of a porous medium, Stud. Appl. Math. 50, 93 (1971)
24. B Jeffrey, H S Udaykumar and K S Schulze, Flow fields generated by peristaltic reflex in isolated guinea pig ileum, Am. J. Physiol. Gastrointest. Liver Physiol. 285, G907 (2003)
25. E F Elshehawey, N T Eldabe, E M Elghazy and A Ebaid, Peristaltic transport in an asymmetric channel through a porous medium, Appl. Math. Comput. 182, 140 (2006)
26. D Tripathi and O Anwar Beg, Magnetohydrodynamic peristaltic flow of a couple stress fluid through coaxial channels containing a porous medium, J. Mech. Med. Biol. 12(5), 1250088(2012)
27. A. Bejan, A study of entropy generation in fundamental convective heat transfer, J. Heat transf. 101 (1979) 718.
28. M. Pakdemirli and B.S. Yilbas, Entropy generation in a pipe due to non-newtonian fluid flow, Indian Academy of Sciences, Sadhana 31 (2006) 21.
29. E. Abu Nada, Entropy generation due to heat and fluid flow in backward facing step flow with various expansion ratios, Int. J. Energy 3 (2006)
30. H. F. Oztop, A. Z. Sahin and I. Dagtekin, Entropy generation through hexagonal cross-sectional duct for constant wall temperature in laminar flow, Int. J. Energy Res. 28 (2004) 725.

31. I. Dagtekin, H. F. Oztop and A. Z. Sahin, A analysis of entropy generation through circular duct with different shaped longitudinal fins of laminar flow, Int. J. Heat Mass transf. 48 (2005) 171.

32. T. Basak, R. Anandalakshmi, P. Kumar and S. Roy, Entropy generation vs. Energy flow due to natural convection in a trapezoidal cavity with isothermal and non-isothermal hot bottom wall, Energy 37 (2012) 514.

33. I. Dagtekin, H .F. Oztop and A. Bahloul, Entropy generation for natural convection in ʃ-shaped enclosures, Int. Commun. Heat Mass 34 (2007) 502.

34. H. F. Oztop and K. Al-Salem, Entropy generation in natural and mixed convection heat transfer for energy systems,Ren. Sust. En. Reviews 16 (2012) 911.

35. R. Ellahi, M. Hassan and A. Zeeshan, Shape effect of nanosize particles in Cu-H2O nanofluid on entropy generation, Int. J. Heat Mass transf. 81 (2015) 449

36. N. S. Akbar, Entropy generation analysis for a CNT suspension Nanofluid in plumb ducts with peristalsis, Entropy 17 (2015) 1411

37. R. Ellahi, Shafiq Ur Rahman, S. Nadeem and K Vafai, The blood flow of prandtl fluid through a tapered stenosed arteries in permeable walls with magnetic field, Commun. Theor. Phys. 63 (2015) 353

38. N. S. Akbar, Entropy generation and energy conversion rate for the peristaltic flow in a tube with magnetic field, Energy 82 (2015) 23

39. R. Ellahi, M. M. Bhatti, C. Fetecau and K. Vafai , Peristaltic flow of couple stress fluid in a non-uniform rectangular duct having compliant walls, Commun. Theor. Phys. 65 (2016) 66

40. N. S. Akbar, Biofluidics study in digestive system with thermal conductivity of shape nanosize H2O+Cu nanoparticles , J. Bionic Eng. 12 (2015) 656

41. N. S. Akbar, A new thermal conductivity model with shaped factor ferromagnetism nanoparticles study for the blood flow in non-tapered stenosed arteries, IEEE Trans. NanoBioscience 14 (2015) 780

42. R. Ellahi, S U Rehman, S Nadeem and Noreen Sher Akbar, Influence of heat and mass transfer on micropolar fluid of blood flow through a tapered stenosed arteries with permeable walls, J. Comput. Theor. Nanosci. 11, 1156 (2014)

43. S Nadeem and H Sadaf, Ciliary motion phenomena of viscous nanofluid in curved channel, Trans. Nanobiosci. 14, 447 (2015)

44. Noreen Sher Akbar and Z H Khan, Influence of magnetic field and slip on jeffrey fluid in a ciliated symmetric channel with metachronal wave pattern, Int. J. Biomath. 8(2), 1550026 (2015)
45. N. S. Akbar, Peristaltic flow with thermal conductivity of H2O+Cu,Int. J. Biomath. 8(2), 1550023 (2015)
46. S Nadeem and H Sadaf, Ciliary motion phenomenon of viscous nanofluid in a curved channel, Eur. Phys. J. - Plus (EPJ Plus) 131, 65 (2016)
47. N. S. Akbar, Physical hydrodynamic propulsion model study on creeping viscous flow through a ciliated porous tube, Pramana - J. Phys. (2017)